

MAGNETIC ORDERING AND SPIN WAVE DYNAMICS IN TRANSITION METAL
ARSENIDES

Draft of December 2, 2020 at 02:12

BY

MANOHAR H. KARIGERASI

DISSERTATION

Submitted in partial fulfillment of the requirements
for the degree of Doctor of Philosophy in Materials Science and Engineering
in the Graduate College of the
University of Illinois at Urbana-Champaign, 2021

Urbana, Illinois

Doctoral Committee:

Associate Professor Daniel P. Shoemaker, Chair
Professor David G. Cahill
Professor Jian-Min Zuo
Research Assistant Professor Gregory MacDougall

Abstract

Metallic antiferromagnets have gained interest in recent times due to the possibility of being useful as a memory device. Arsenic forms a large pool of magnetic metals in combination with other transition metals that have largely been ignored so far. In this report, we discover a new ternary metallic arsenide in the Cu-Mn-As phase space, identify its chemical and magnetic structure, and characterize its electrical and magnetic properties. We also carry out the magnetic structure refinement of Mn_3As_2 from neutron powder diffraction data at different temperatures to understand the magnetic ordering in Mn-As compounds. Using inelastic neutron scattering measurements, we determine exchange interactions in Fe_2As , which has the same structure as CuMnAs, showing a highly 2D magnon character although the phonons are 3D. Finally, we report a magnetic-structural coupled transition across 300 K in tetragonal CuMnAs and determine the correct magnetic structure of the compound.

Acknowledgments

This project would not be possible without many people. Firstly, thanks to my advisor, Prof. Daniel P. Shoemaker.

Table of Contents

List of Tables	v
List of Figures	vi
Chapter 1 Introduction	1
1.1 Magnetic information storage	1
1.2 Antiferromagnets for potential applications as a memory unit	2
1.3 Exploration of Cu-Mn-As phase space	2
1.4 Exchange interactions in Cu ₂ Sb type structures	5
Chapter 2 Theory of electrical switching in metallic antiferromagnets	6
2.1 Hidden spin polarization in centrosymmetric crystals	6
2.2 Finding metallic antiferromagnetic candidates with R2-D2 effect	7
2.3 Components of torque from non-equilibrium CISP	9
2.4 Spin polarization in CuMnAs, Mn ₂ Au and Fe ₂ As	11
2.5 Conclusions	12
2.6 Acknowledgements	15
Chapter 3 Materials synthesis and characterization	16
3.1 Bulk materials synthesis	16
3.1.1 Sensitivity of Fe:As stoichiometry in the synthesis of Fe ₂ As	16
3.2 Synthesis of compounds in the Cu-Mn-As system	18
3.3 Materials characterization	19
3.3.1 X-ray diffraction	19
3.3.2 Calorimetry	20
3.3.3 SQUID magnetometry	21
3.3.4 Transport measurements	22
3.4 Neutron scattering	22
3.4.1 Neutron powder diffraction	22
3.4.2 Inelastic neutron scattering	22

Chapter 4 Magnetic structure refinement from neutron diffraction measurements	23
Chapter 5 Discovery and magnetic frustration of hexagonal Cu_{0.82}Mn_{1.18}As	29
Chapter 6 Two step magnetic ordering in monoclinic Mn₃As₂	38
Chapter 7 Spin canting in tetragonal CuMnAs	48
Chapter 8 Exchange interactions in Fe₂As probed by inelastic neutron scattering	50
Chapter 9 Conclusions	59
References	61

List of Tables

2.1	Different cases of spin polarization depending on the symmetry of atomic sites and the unit cell [26].	7
2.2	List of metallic antiferromagnetic candidates filtered out from MPDS and ASM database and their metal atom site symmetries	9
2.3	Summary of the linear response tensor components for the CISP observable and electric field	11
2.4	Linear response tensor in CuMnAs and Mn ₂ Au assuming Mn moment to be 1 μ_B	13
2.5	Linear response tensor in Fe ₂ As when Fe moments have been set to 0 μ_B	14

List of Figures

1.1	The magnetic structures of tetragonal CuMnAs and MnF ₂ are shown in (a) and (b), respectively.	3
1.2	Magnetic structure of orthorhombic CuMnAs	3
1.3	Cu-Mn-As ternary phase diagram highlighting some of the known ternary compounds in blue and known magnetic structures in red. Not all compounds in this system are shown here.	4
2.1	The schematic of the Fermi surface of the local sectors near Mn1 and Mn2 atoms are shown in (a) and (b), respectively. The magnetic structure of tetragonal CuMnAs is shown in (c) which also includes the highlighted local sectors.	7
2.2	Magnetic structure of Fe ₂ As along with the Fe site numbers corresponding to Table 2.5.	12
3.1	The process of making bulk materials using traditional solid state synthesis technique is shown here. The powders mixed inside the glovebox in (a) are transferred to a quartz tube and vacuum sealed in (b). The vacuum sealed ampoule in (c) is placed inside the box furnace in (d) and subjected to a heating profile. (e) shows the final ingot obtained in case of CuMnAs sample.	17
3.2	Impurity percentage as a function of Fe:As starting stoichiometry ratio with 200 mesh size Fe powders for making Fe ₂ As samples.	17
3.3	Synchrotron x-ray diffraction data of Fe ₂ As for different ratios of Fe:As from 10 μm Fe powders is shown in (a) and the corresponding impurity percentage is shown in (b).	18
3.4	The flat-bottom bulk of the quartz ampoules is shown in (a) and (b) shows the final powder-containing vacuum sealed ampoules.	21
4.1	Electronic band structure	24
4.2	Electronic band structure	24
4.3	Electronic band structure	25
4.4	Electronic band structure	25
4.5	Electronic band structure	26
4.6	Electronic band structure	27
4.7	Electronic band structure	27
5.1	Electronic band structure	30
5.2	Electronic band structure	31
5.3	Electronic band structure	32

5.4	Electronic band structure	33
5.5	Electronic band structure	34
5.6	Electronic band structure	34
5.7	Electronic band structure	35
5.8	Electronic band structure	35
5.9	Electronic band structure	36
6.1	Electronic band structure	39
6.2	Electronic band structure	40
6.3	Electronic band structure	41
6.4	Electronic band structure	42
6.5	Electronic band structure	43
6.6	Electronic band structure	44
6.7	Electronic band structure	45
6.8	Electronic band structure	46
6.9	Electronic band structure	47
8.1	Electronic band structure	51
8.2	Electronic band structure	51
8.3	Electronic band structure	52
8.4	Electronic band structure	53
8.5	Electronic band structure	54
8.6	Electronic band structure	54
8.7	Electronic band structure	55
8.8	Electronic band structure	55
8.9	Electronic band structure	56
8.10	Electronic band structure	56
8.11	Electronic band structure	57
8.12	Electronic band structure	57

Chapter 1

Introduction

1.1 Magnetic information storage

2 In information memory storage devices, there is typically a trade-off between the optimum
3 speed or response time and the complexity and size of memory storage [1]. Volatile memory
4 refers to temporary memory storage where the data is lost when the power is removed.
5 Volatile memory such as SRAM (static random access memory) and DRAM (dynamic random
6 access memory) are used as CPU caches and main memory respectively. SRAM has much
7 faster access times and does not require periodic refreshing. However, it requires four to six
8 transistors per bit as compared to one transistor and one capacitor in DRAM devices [2]. Non-
9 volatile memory (NVM) storage devices on the other hand, retain their data for a long period
10 of time until perturbed. Modern computers mostly use flash memory based solid state drives
11 (SSD) and magnetic hard disk drives (HDD) for storing large amounts of data permanently [2].
12 The first HDD was invented in 1956 by IBM and since then, has seen more than eight orders of
13 magnitude improvement in the storage density. However, the trilemma in magnetic recording
14 between poor thermal stability, coercive fields and signal-to-noise ratio has resulted in the
15 HDD reaching a saturation limit in their device performance [3]. Flash memory uses floating
16 gate MOSFETs (metal oxide semiconductor field effect transistors) to store memory and does
17 not contain any moving parts. Although SSD have dominated the NVM marketshare last few
18 years, there is an increasing need for alternative NVM technologies that are fast, low power
19 consuming and have high storage density [2].

20 One such emerging NVM is MRAM (magnetoresistive random access memory). Unlike
21 flash memory which uses electronic charge as a medium of memory storage, MRAM uses the
22 electronic spin degree of freedom to store information. Unlike charge based storage devices,
23 MRAM is stable against perturbations such as ionizing radiation [4]. MRAM devices consist
24 of cells with magnetic tunnel junctions (MTJ) that have two ferromagnet (FM) layers separated
25 by an insulating layer. One of the layer is pinned where the magnetization orientation is fixed
26 and acts as a reference layer. Depending on the orientation of the free layer, the tunneling
27 magnetoresistance (TMR) is high or low and hence, memory can be read out using electrical
28 currents [3]. Early MRAMs were written by induced fields from heavy currents passed on
29 the adjacent layer. With recent developments in spin transfer torque (STT) in ferromagnets,

30 it has become possible to write using electrical currents [5]. This has reduced the power
31 consumption significantly and made commercialization of MRAM devices possible [3,6].

32 **1.2 Antiferromagnets for potential applications as a memory unit**

33 Historically, antiferromagnets (AFM) have been used as inactive components in MTJ, primarily
34 in exchange biasing the pinned FM layer. However in 2010, Gomonay *et al.* [7] proposed
35 electrical switching of AFMs using STT by passing a spin polarized current injected from
36 a fixed FM layer through the AFM layer. The electrical current gets spin polarized in the
37 FM layer and transfers its angular momentum to the AFM moments to switch it from one
38 orientation to another. There are advantages to using AFM over FM in MRAM devices. AFM
39 are not easily affected by external magnetic fields and do not produce stray fields of their
40 own. They have smaller domains which would allow for higher storage densities [4]. Since
41 the precession frequency of AFM moments is determined the geometric mean of exchange
42 and anisotropy energies, the dynamics in AFM materials occur at THz timescales which is
43 two orders of magnitude higher than in FM [8]. Although the AFM can be switched using
44 electrical currents from parallel to perpendicular orientation with respect to the FM mag-
45 netization direction, the reverse process cannot be obtained using electrical current. High
46 magnetic fields above the spin flop transition of the AFM needs to be applied in order to
47 switch back the AFM to its original state [7].

48 Unlike previously discussed STT MRAM devices, spin orbit torque based electrical switch-
49 ing in broken inversion symmetry FM does not require the presence of a FM polarizer [9].
50 This concept of the presence of relativistic fields is applicable to AFM as well provided the
51 local moments do not sit on centrosymmetric sites. If the two sublattices are related to each
52 other by a center of inversion, then the current induced spin polarized fields are staggered
53 across the two sublattices [4,10,11]. This results in a uniform fieldlike torque experienced by
54 the order parameter. This is possible in bulk materials that are globally centrosymmetric but
55 locally non-centrosymmetric and the two sublattices are related to each other by a center of
56 inversion. It was initially demonstrated in the case of epitaxially grown tetragonal CuMnAs
57 thin films on GaP substrate [4] and since then, it has also been shown in Mn₂Au and CuMnAs
58 sputtered films as well [12,13]. Observation of electrical switching behavior in AFM requires
59 the presence of degenerate Néel vectors like in CuMnAs as shown in Fig. 1.1(a) as opposed to
60 compounds like MnF₂ where the Mn moments point along *c* in Fig. 1.1(b).

61 **1.3 Exploration of Cu-Mn-As phase space**

62 Compounds in Cu-Mn-As phase space have attracted a lot of attention in recent times mainly
63 due to the exotic properties of tetragonal and orthorhombic CuMnAs. As mentioned earlier,

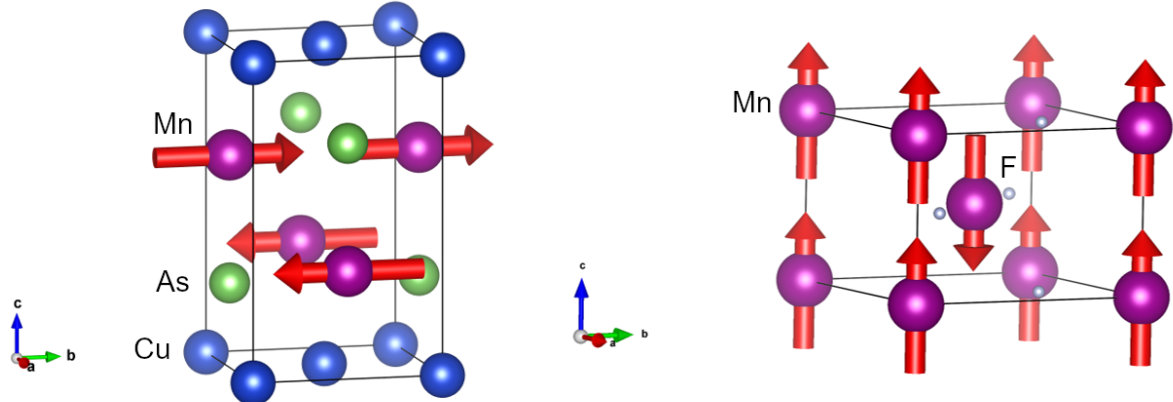


Figure 1.1: The magnetic structures of tetragonal CuMnAs and MnF₂ are shown in (a) and (b), respectively.

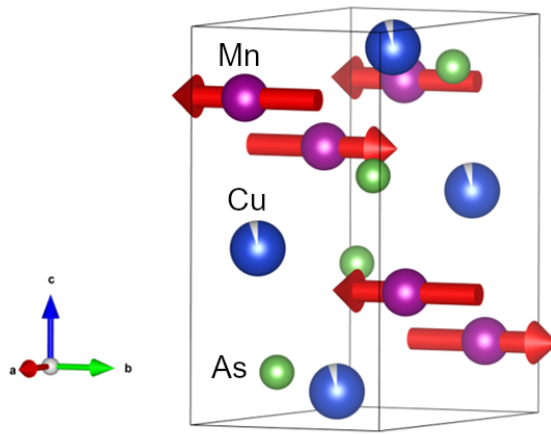


Figure 1.2: Magnetic structure of orthorhombic CuMnAs

tetragonal CuMnAs was the first antiferromagnet where electrical switching was supposedly demonstrated. Orthorhombic CuMnAs, shown in Fig. 1.2, was the first magnetic compound to be proposed as a Dirac semimetal. It is a special compound where the inversion and time reversal symmetry of the magnetic structure is broken but their combined symmetry (*PT* symmetry) is still preserved. Based on the orientation of the AFM order parameter, the compound changes from a conducting to an insulating phase. Hence, there are voltage based switching applications that have been proposed for this compound [14].

Despite the growing importance of the compounds in Cu-Mn-As system, the Cu-Mn-As ternary phase space has not been explored properly. There are four known ternary compounds including both the polymorphs of CuMnAs, orthorhombic CuMn₃As₂ and Cu₂Mn₄As₃ as shown in Fig. 1.3 [15–18]. Bulk orthorhombic CuMnAs can be grown us-

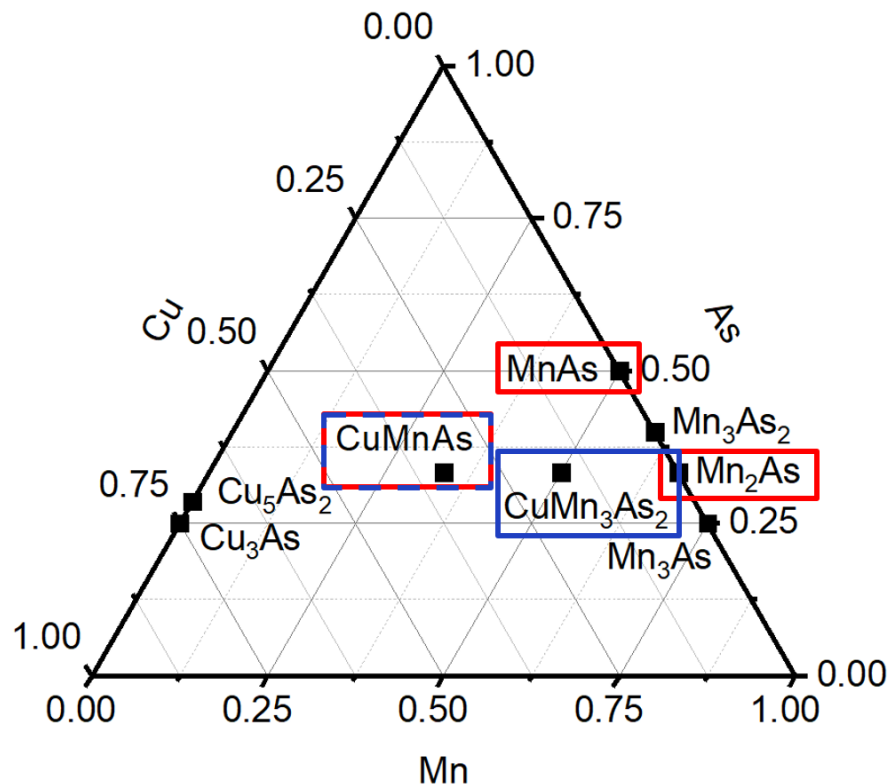


Figure 1.3: Cu-Mn-As ternary phase diagram highlighting some of the known ternary compounds in blue and known magnetic structures in red. Not all compounds in this system are shown here.

75 ing traditional solid state synthesis routes by Cu, Mn and As powders in stoichiometric ratio
76 and heating the powders to 1000°C. In order to synthesize pure bulk tetragonal CuMnAs,
77 we have to go off-stoichiometry and either substitute Mn with Cu or As [18]. Hence, it is
78 important to explore different regions in the Cu-Mn-As system and verify the stability of
79 different ternary compounds. The magnetic structures in the Cu-Mn-As system have also
80 not been identified for most of the compounds. Apart from the four Cu-Mn-As ternary
81 compounds, there are more than ten Mn-As binary compounds present in this system. The
82 magnetic structures are known only for the two previously mentioned CuMnAs compounds,
83 Mn₂As and MnAs as shown in Fig. 1.3 [16,17,19–22]. Since most, if not all, the binary Mn-As
84 compounds are metallic, there is a need to magnetically characterize the compounds and
85 identify their magnetic structures.

86 1.4 Exchange interactions in Cu₂Sb type structures

87 If we want to understand the electrical switching behavior in metallic antiferromagnets, we
88 should be able to quantify the fundamental energies such as magnetocrystalline anisotropy
89 and exchange interactions in materials like CuMnAs. CuMnAs has a Cu₂Sb structure type.
90 Other materials with this structure includes Mn₂As, Cr₂As, Fe₂As, CrMnAs, MnFeAs etc.
91 [23–25]. Although Mn₂As, Cr₂As and Fe₂As have the same structure, the magnetic ground
92 state is different in all three compounds. The strength and sign of direct exchange interactions
93 between two magnetic atoms is a result of the nature of orbital overlap between the two
94 magnetic atoms [24]. Since these materials are metallic, there are two contributions to indirect
95 exchange interactions. One contribution arises from superexchange interactions mediated by
96 As atoms and the other contribution comes from RKKY (Ruderman–Kittel–Kasuya–Yosida)
97 interactions [25]. It is important that we are able to determine what spin interactions are
98 relevant and how does it affect the magnetic ordering in these materials. It is also crucial that
99 we are able to verify the computational methods and the exchange coupling values obtained
100 from these methods so that we can use these methods for other systems as well.

Chapter 2

Theory of electrical switching in metallic antiferromagnets

101 Electrical switching in any magnetic compound is a series of events involving current induced
102 spin polarization (CISP) of charge carriers and different components of CISP exerting differ-
103 ent torque on the magnetic moments of the atoms. The nature of CISP is set by the crystal
104 symmetry. In previous studies of CuMnAs and Mn₂Au, it was stated that the compound
105 should globally centrosymmetric but locally non-centrosymmetric and the two sublattices
106 should be related to each other by a center of inversion [4,10,11]. Is this a necessary condition
107 for observing a staggered spin polarization configuration and can it be applied to general
108 cases? These are some of the questions we will answer in this chapter. Once we have deter-
109 mined the required symmetry criteria, we will filter out metallic antiferromagnetic candidates
110 from large databases of materials such as MPDS (Materials Platform for Data Science) and
111 ASM (ASM International), and analyze the effect of CISP on the torque experienced by the
112 order parameter.

113 2.1 Hidden spin polarization in centrosymmetric crystals

114 It has been known for quite some time that in materials (even non-magnetic) having large
115 spin orbit coupling (SOC) and lacking a center of inversion, magnetic fields are induced.
116 When materials possess structural inversion asymmetry such as in quantum wells and other
117 heterostructures, this effect is called the Rashba effect and it results in a helical type spin
118 texture. When this occurs in materials that lack bulk inversion symmetry, the effect is called
119 the Dresselhaus effect and it results in a unique spin texture [26]. Zhang *et al.* [26] argued that
120 since SOC is a relativistic effect, instead of considering the symmetry of the entire unit cell,
121 one should check for atomic site symmetry to understand SOC induced spin polarization.
122 Based on this argument, there are four cases possible as shown in Table 2.1.

123 R1 and D1 effects refer to conventional Rashba and Dresselhaus spin polarization respec-
124 tively. In materials that are globally centrosymmetric, hidden spin polarization is possible.
125 There is local spin polarization near non-centrosymmetric sites but when summed over the
126 entire unit cell, the net spin polarization is zero. This effect is called the R2 or D2 effect
127 corresponding to Rashba or Dresselhaus effect, respectively in centrosymmetric crystals. The
128 total spin polarization of the unit cell is the vector sum of all the local spin polarizations

Table 2.1: Different cases of spin polarization depending on the symmetry of atomic sites and the unit cell [26].

	All non-polar point groups	At least one polar point groups	All centrosymmetric point groups
Non-Centrosymmetric space group	D1 effect	R1/D1 effect	Not possible
Centrosymmetric space group	D2 effect	R2/D2 effect	No spin polarization

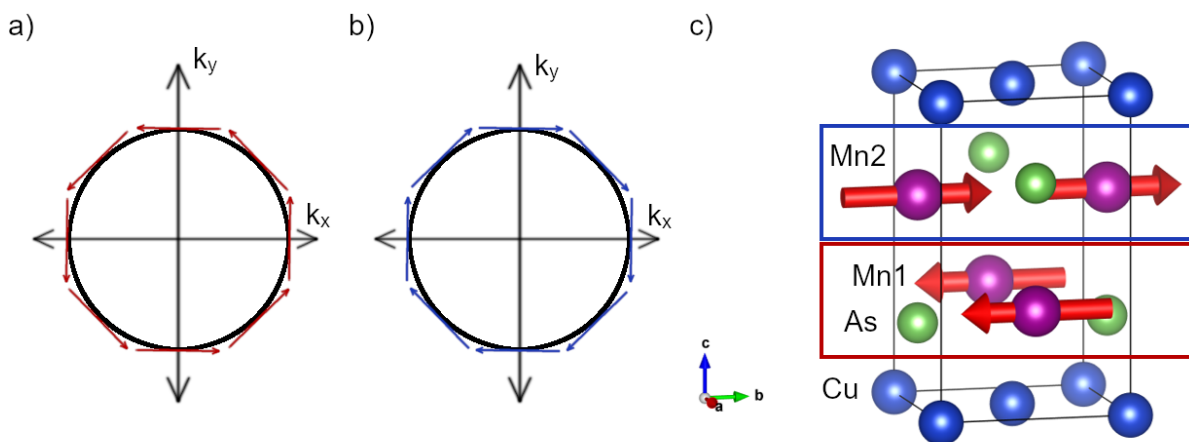


Figure 2.1: The schematic of the Fermi surface of the local sectors near Mn1 and Mn2 atoms are shown in (a) and (b), respectively. The magnetic structure of tetragonal CuMnAs is shown in (c) which also includes the highlighted local sectors.

129 in the unit cell. Non-centrosymmetric point groups can be further divided into polar and
 130 non-polar groups. Local Rashba effect requires the presence of polar point groups on atomic
 131 sites and the local Dresselhaus effect requires the presence of non-polar point groups at the
 132 atom sites. The presence of local spin polarization in centrosymmetric crystals opens the
 133 avenue for studying spin polarization in a larger group of compounds including metallic
 134 antiferromagnets.

135 2.2 Finding metallic antiferromagnetic candidates with R2-D2 136 effect

137 In spin orbit torque based switching of metallic antiferromagnets, the same arguments apply
 138 as before except that we only care about the point group symmetry at the magnetic atom
 139 sites. For example, the magnetic structure of CuMnAs is shown in Fig. 2.1(c). Cu and As

140 atoms have no moments and sit on D_{2d} and C_{4v} sites, respectively. Since only the Mn atoms
141 have moments, we must take the site symmetry of Mn atoms into consideration. Mn atom
142 sites have C_{4v} point group symmetry which is polar. As seen in Fig. 2.1(a,b), the schematic
143 of the Fermi surface corresponding to the Mn layer has a Rashba-like spin texture. When
144 the current is applied, through inverse spin galvanic effect, there is a spin polarization of
145 the conduction electrons near Mn sites. The spin polarization is staggered across the two
146 Mn sublattices and through exchange coupling, a torque is experienced by the Mn moments.
147 From the example of CuMnAs above, we can search for compounds from databases that are
148 antiferromagnets or are likely to be antiferromagnets where the magnetic atoms sit on a polar
149 point group. Such a search can be made for compounds which are not complicated by the
150 presence of many magnetic sites with different point groups. The general case applicable for
151 all magnetic compounds will be considered in the following sections. Following is the general
152 procedure for extracting potential metallic antiferromagnet candidates from databases -

- 153 1. Search for known metallic antiferromagnets from database having tetragonal, trigonal
154 or hexagonal crystal system.
- 155 2. Remove duplicate and non-centrosymmetric compounds.
- 156 3. Identify the Néel temperature and magnetic ordering.
- 157 4. Filter out compounds having Néel temperature > 300 K.
- 158 5. Identify the nature of atomic site symmetry and select compounds.
- 159 6. Study available literature to see if any compounds can be synthesized as single crystals.

160 This procedure assumes that we are starting with a collection of known or possible metallic
161 antiferromagnets. This is true in case of compounds downloaded from MPDS. In case of ASM
162 database, the compounds are metallic but their magnetism is not known beforehand. We will
163 have to make some assumptions based on the chemical nature and stoichiometry of the ions
164 present in the compound in order to select possible antiferromagnets. Tetragonal, trigonal
165 or hexagonal crystal systems are preferred since they allow for the presence of multiple
166 degenerate axes for Néel vector orientation. It is still important to check if the magnetic
167 structure for the compound is known or not and if the Néel vector points along the degerate
168 axes. Carrying out the above mentioned steps for compounds in MPDS and ASM database
169 gives us a list of compounds in Table 2.2 that have been grouped together based on their
170 structure types.

171 The first group of compounds consist of materials in MoSi_2 structure type. Mn_2Au is a
172 well-known compound that has been extensively studied for electrical switching applications
173 [12, 27]. Cr_2Al powders can be prepared using traditional solid state synthesis routes by
174 heating to above 850°C [28]. Early neutron diffraction experiments suggest Cr moments align

Table 2.2: List of metallic antiferromagnetic candidates filtered out from MPDS and ASM database and their metal atom site symmetries

Structure type	List of compounds	Point group	Magnetism
MoSi ₂	Mn ₂ Au, Cr ₂ Al, Ni ₂ Ta	C _{4v}	Mn ₂ Au is a known candidate
HfFe ₆ Ge ₆	ScFe ₆ Ge ₆	C _{2v}	AFM with Néel vector along <i>c</i>
Mg ₃ Cd	Mn ₃ Ga, Mn ₃ Ge, Mn ₃ Sn, Fe ₃ Ga, Co ₃ Mo, Co ₃ W, Ni ₃ In, Ni ₃ Sn, Ni ₃ Zr	C _{2v}	Non-collinear AFM
IrIn ₃	CoGa ₃ , CoIn ₃ , FeGa ₃	C _{2v}	FeGa ₃ and CoGa ₃ are diamagnets
MoNi ₄	MoNi ₄ , WNi ₄	C _{1v}	Unknown
Ni ₂ Al ₃	Ni ₂ Al ₃ , Ni ₂ Ga ₃ , Ni ₂ In ₃	C _{3v}	Unknown

at 65° to the *ab* plane [29]. However, a later article indicates that the determined magnetic structure may not be correct [30]. Regardless of whether the moments align in the *ab* plane or not, Cr₂Al is an interesting candidate to study electrical switching behavior. ScFe₆Ge₆ is AFM at room temperature [31]. However, the Fe moments align along *c* and does not satisfy our criteria [32]. Compounds in the Mg₃Cd structure type contain Kagome lattice of magnetic atoms. Mn₃Sn and Mn₃Ge are known to have a non-collinear spin arrangement. They have become popular recently for showing large anomalous hall and spin hall effect behavior [33–35]. Electrical switching was also demonstrated in Mn₃Sn recently. In the fourth group of compounds, both FeGa₃ and CoGa₃ are known to show diamagnetic properties and hence they can be discarded [36–38]. The magnetism is unknown in the final two groups of compounds in MoNi₄ and Ni₂Al₃ structure types and most of these compounds can be synthesized by the arc melting process [39,40].

2.3 Components of torque from non-equilibrium CISP

The previous section dealt with relatively simple magnetic compounds that had only one magnetic atom site and we were concerned with the point group of the site to determine whether the inverse spin galvanic effect would be observed or not. In the simplest sense, antidamping-like STT is induced by spin hall effect (SHE) and fieldlike SOT is generated from inverse spin galvanic effect. However, incomplete absorption of the spin current from SHE by the FM layer may produce a fieldlike torque, and spin relaxation and damping may induce an antidamping like component to the SOT [11]. Using Kubo linear formalism, we

195 can write CISP $\delta S_a = \chi_a E$ where E is the applied electric field and χ_a is the linear response
 196 tensor for the sublattice a. χ_a can be further divided into three components:

$$\chi_a = \chi_a^I + \chi_a^{II(a)} + \chi_a^{II(b)} \quad (2.1)$$

197 where χ_a^I is the intraband term, and $\chi_a^{II(a)}$ and $\chi_a^{II(b)}$ are the interband terms. χ_a can also
 198 be broken down into even and odd terms:

$$\chi_a = \chi_a^{even} + \chi_a^{odd} \quad (2.2)$$

199 where $\chi_a^{even} = (\chi_a([M]) + \chi_a([-M]))/2$ and $\chi_a^{odd} = (\chi_a([M]) - \chi_a([-M]))/2$. From the
 200 symmetry of the operators and the matrix element, it follows that -

$$\chi_a^{even} = \chi_a^I + \chi_a^{II(b)} \quad (2.3)$$

$$\chi_a^{odd} = \chi_a^{II(a)} \quad (2.4)$$

201 We assume that the system only has a weak disorder and hence, we can neglect $\chi_a^{II(b)}$. χ_a
 202 also depends on the direction of the magnetic moments where \hat{n} is the direction of the Néel
 203 vector.

$$\chi_{a,i,j}(\hat{n}) = \chi_{a,i,j}^{(0)} + \chi_{a,i,j,k}^{(1)} \hat{n}_k + \chi_{a,i,j,k,l}^{(2)} \hat{n}_k \hat{n}_l + \dots \quad (2.5)$$

204 where the sum of the first term and every alternate term after that corresponds to χ_a^{even} and
 205 the sum of the remaining terms correspond to χ_a^{odd} . $\chi_a^{(0)}$ is usually dominant, independent
 206 of magnetization and contributes to field-like torque. $\chi_a^{(1)}$ contributes to anti-damping like
 207 torque and $\chi_a^{(2)}$ can be neglected if $\chi_a^{(0)}$ is not 0 [11]. The zeroth order term which contributes
 208 to a fieldlike torque consists of three components in the form of generalized Rashba and
 209 generalized Dresselhaus terms and a term that is proportional to the electric field as shown
 210 by the following equations:

$$\text{Generalized Rashba } \chi_a^{gR} = \begin{bmatrix} \chi_{11} & -\chi_{21} & 0 \\ \chi_{21} & \chi_{11} & 0 \\ 0 & 0 & 0 \end{bmatrix} \quad (2.6)$$

$$\text{Generalized Dresselhaus } \chi_a^{gD} = \begin{bmatrix} \chi_{11} & \chi_{21} & 0 \\ \chi_{21} & -\chi_{11} & 0 \\ 0 & 0 & 0 \end{bmatrix} \quad (2.7)$$

Table 2.3: Summary of the linear response tensor components for the CISP observable and electric field

	χ_a^I	$\chi_a^{II(a)}$	$\chi_a^{II(b)}$
Component	Intraband	Interband (imaginary)	Interband (real)
Disorder $\Gamma \rightarrow 0$	Diverges	Constant	Zero
Cause	Non-equilibrium Fermi-Dirac distribution	Intrinsic change in carrier wave function	Change in carrier wave function due to disorder/defects
Alternate name	χ_a^{even} or $\chi_a^{(0)}$	χ_a^{odd} or $\chi_a^{(1)}$	
Dependence on magnetization	Independent	Dependent	
Torque	Field-like	Anti-damping-like	

$$\text{Proportional to Electric field } \chi_a^E = \begin{bmatrix} \chi_{11} & 0 & 0 \\ 0 & \chi_{11} & 0 \\ 0 & 0 & \chi_{11} \end{bmatrix} \quad (2.8)$$

211 Similarly, the first order term can also be broken into three different components [11]. The
 212 summary of the linear response tensor components is also provided in the Table 2.3

213 2.4 Spin polarization in CuMnAs, Mn₂Au and Fe₂As

214 Zelezny *et al.* [11] provides a python code *symmetr* for analyzing the linear response tensor
 215 for a number of observables such as current, spin, torque, position, spin current etc. and
 216 electric field. Using this code, we can test the reponse tensor of known compounds such
 217 as CuMnAs and Mn₂Au and also check for unknown compounds such as Fe₂As. Table
 218 shows the linear response tensor in case of CuMnAs or Mn₂Au. Both compounds have
 219 same spin polarization since they are both globally centrosymmetric and Mn atoms sit on
 220 C_{4v} point group sites. Let us first understand χ^{even} for all the different cases presented here.
 221 Magnetism can be turned off to avoid including magnetization-based effects to the reponse
 222 tensor. Regardless of whether we toggle magnetism in Mn atoms or not, χ^{even} is 0 for the
 223 whole unit cell since it is centrosymmetric. When Mn magnetic moment is set to 0, χ^{even} for
 224 each sublattice corresponds to the response in conventional Rashba spin texture. Regardless
 225 of magnetism, the spin polarization in one site is opposite to that of another site as seen in
 226 the projected cases. When magnetism is turned on, $|\chi_{10}| = |\chi_{01}|$ is not valid anymore since
 227 we also have to consider higher terms in χ^{even} . In case of χ^{odd} , it is 0 when magnetization is

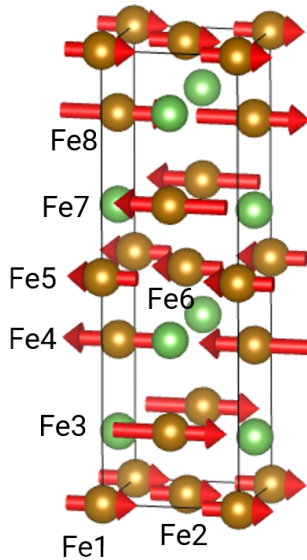


Figure 2.2: Magnetic structure of Fe_2As along with the Fe site numbers corresponding to Table 2.5.

228 turned off as also shown in Table 2.3. When magnetic moments are allowed, there is spin
229 polarization along c direction.

230 Table 2.5 shows linear response tensor components in Fe_2As . Fe_2As is complicated by the
231 presence of two different Fe sites. $\text{Fe}1$, $\text{Fe}2$, $\text{Fe}5$ and $\text{Fe}6$ atoms shown in Fig. 2.2 sit on D_{2d}
232 site whereas $\text{Fe}3$, $\text{Fe}4$, $\text{Fe}7$ and $\text{Fe}8$ atoms sit on C_{4v} sites. The table only shows cases where
233 Fe moments have not been considered. However, the results with finite Fe moments in case of
234 χ^{even} can be easily inferred from this table by removing the equality between the magnitudes
235 of χ_{ij} and χ_{ji} . As expected, χ^{odd} is a zero matrix when magnetism is turned off. χ^{even} is 0
236 when the entire unit cell is considered which is expected since the unit cell is centrosymmetric
237 like in the previous case. The sublattices $\text{Fe}3$ and $\text{Fe}4$ sitting on polar point groups show
238 conventional Rashba spin polarization behavior. When χ^{even} at $\text{Fe}3$ is projected onto $\text{Fe}4$, we
239 can see that the response is exactly opposite to $\text{Fe}4$. In case of sublattices $\text{Fe}1$ and $\text{Fe}2$ sitting
240 on non-polar point groups, χ^{even} corresponds to generalized Dresselhaus polarization when
241 χ_{00} and χ_{11} have been set to 0. As expected, the spin polarization would be opposite on the
242 two sublattices. The nature of χ^{odd} when magnetism is included has not been discussed here.

243 2.5 Conclusions

244 There can be local spin polarization present even in centrosymmetric crystals provided the
245 unit cell contains non-centrosymmetric point groups. In CISP based switching, it is important
246 that the magnetic ions sit on non-centrosymmetric sites. The presence of polar point group

Table 2.4: Linear response tensor in CuMnAs and Mn₂Au assuming Mn moment to be 1 μ_B .

	χ^{even}	χ^{odd}
Magnetic Mn. For the entire unit cell	$\begin{bmatrix} 0 & 0 & 0 \\ 0 & 0 & 0 \\ 0 & 0 & 0 \end{bmatrix}$	$\begin{bmatrix} 0 & 0 & \chi_{02} \\ 0 & 0 & 0 \\ \chi_{20} & 0 & 0 \end{bmatrix}$
Magnetic Mn. For each Mn sublattice	$\begin{bmatrix} 0 & \chi_{01} & 0 \\ \chi_{10} & 0 & 0 \\ 0 & 0 & 0 \end{bmatrix}$	$\begin{bmatrix} 0 & 0 & \chi_{02} \\ 0 & 0 & 0 \\ \chi_{20} & 0 & 0 \end{bmatrix}$
Magnetic Mn. For one Mn sublattice projected onto another	$\begin{bmatrix} 0 & -\chi_{01} & 0 \\ -\chi_{10} & 0 & 0 \\ 0 & 0 & 0 \end{bmatrix}$	$\begin{bmatrix} 0 & 0 & \chi_{02} \\ 0 & 0 & 0 \\ \chi_{20} & 0 & 0 \end{bmatrix}$
Non-magnetic Mn. For the entire unit cell	$\begin{bmatrix} 0 & 0 & 0 \\ 0 & 0 & 0 \\ 0 & 0 & 0 \end{bmatrix}$	$\begin{bmatrix} 0 & 0 & 0 \\ 0 & 0 & 0 \\ 0 & 0 & 0 \end{bmatrix}$
Non-magnetic Mn. For each Mn sublattice	$\begin{bmatrix} 0 & -\chi_{10} & 0 \\ \chi_{10} & 0 & 0 \\ 0 & 0 & 0 \end{bmatrix}$	$\begin{bmatrix} 0 & 0 & 0 \\ 0 & 0 & 0 \\ 0 & 0 & 0 \end{bmatrix}$
Non-magnetic Mn. For one Mn sublattice projected onto another	$\begin{bmatrix} 0 & \chi_{10} & 0 \\ -\chi_{10} & 0 & 0 \\ 0 & 0 & 0 \end{bmatrix}$	$\begin{bmatrix} 0 & 0 & 0 \\ 0 & 0 & 0 \\ 0 & 0 & 0 \end{bmatrix}$

Table 2.5: Linear response tensor in Fe₂As when Fe moments have been set to 0 μ_B .

	χ^{even}	χ^{odd}
For the entire unit cell	$\begin{bmatrix} 0 & 0 & 0 \\ 0 & 0 & 0 \\ 0 & 0 & 0 \end{bmatrix}$	$\begin{bmatrix} 0 & 0 & 0 \\ 0 & 0 & 0 \\ 0 & 0 & 0 \end{bmatrix}$
For Fe1 and Fe2	$\begin{bmatrix} 0 & \chi_{10} & 0 \\ \chi_{10} & 0 & 0 \\ 0 & 0 & 0 \end{bmatrix}$	$\begin{bmatrix} 0 & 0 & 0 \\ 0 & 0 & 0 \\ 0 & 0 & 0 \end{bmatrix}$
For Fe3 and Fe4	$\begin{bmatrix} 0 & -\chi_{10} & 0 \\ \chi_{10} & 0 & 0 \\ 0 & 0 & 0 \end{bmatrix}$	$\begin{bmatrix} 0 & 0 & 0 \\ 0 & 0 & 0 \\ 0 & 0 & 0 \end{bmatrix}$
For Fe1 projected onto Fe2	$\begin{bmatrix} 0 & -\chi_{10} & 0 \\ -\chi_{10} & 0 & 0 \\ 0 & 0 & 0 \end{bmatrix}$	$\begin{bmatrix} 0 & 0 & 0 \\ 0 & 0 & 0 \\ 0 & 0 & 0 \end{bmatrix}$
For Fe3 projected onto Fe4	$\begin{bmatrix} 0 & \chi_{10} & 0 \\ -\chi_{10} & 0 & 0 \\ 0 & 0 & 0 \end{bmatrix}$	$\begin{bmatrix} 0 & 0 & 0 \\ 0 & 0 & 0 \\ 0 & 0 & 0 \end{bmatrix}$
For Fe1 projected onto Fe3	No relation	No relation

247 is required for Rashba spin polarization and non-polar point group for Dresselhaus spin
248 polarization. We need to consider both antidamping-like torque and fieldlike torque when
249 considering spin polarization. In broken inversion symmetry 2D AFM, it is the antidamping-
250 like torque that can provide a mechanism for switching since the fieldlike torque component
251 of CISP is uniform. In Fe₂As, CISP from ISGE in Fe3 and Fe4 sublattices is similar to Mn in
252 CuMnAs. However, there is no relation between the even component of CISP in Fe1 or Fe2
253 and Fe3 or Fe4 sublattices. This allows for two possibilities when the current is along [100].
254 If the torque acts in the same direction for both sets of Fe atoms, then it would provide a
255 possible pathway for switching. However, if the fieldlike torque act in the opposite direction
256 for both sets of Fe moments, then a large current threshold may be required before the
257 moments can be possibly switched.

258 **2.6 Acknowledgements**

259 I would like to acknowledge two REU students, Scott Berens and Carmen Paquette, for
260 compiling the list of metallic antiferromagnets from MPDS and ASM databases respectively.
261 It saved me a lot of time and I was able to analyze the symmetry requirements on a much
262 smaller list of compounds.

Chapter 3

Materials synthesis and characterization

263 3.1 Bulk materials synthesis

264 Bulk polycrystalline and single crystals of all the samples are prepared by traditional solid
265 state synthesis routes. The process of synthesizing these samples is shown in Fig. 3.1. The
266 constituent elements of the compounds are mixed in certain ratio using a mortar and pestle
267 in an Argon atmosphere glovebox shown in Fig. 3.1(a). Quartz tubes, that have been sealed
268 from one side, are filled with the mixed elemental powders and vacuum sealed using a
269 flame torch as shown in Fig. 3.1(b). The sealed quartz tubes in Fig. 3.1(c) are placed inside
270 a box furnace and heated to a high temperature to allow the powders to fuse together as
271 shown in Fig. 3.1(d). Upon cooling, the desired crystal is removed from the quartz tube and
272 characterized.

273 3.1.1 Sensitivity of Fe:As stoichiometry in the synthesis of Fe_2As

274 Fe_2As crystals are prepared by mixing Fe and As powders inside the glovebox and heating
275 it up to 600°C at $1^\circ\text{C}/\text{min}$, holding it for 6 h and then heating it above the melting point to
276 975°C at $1^\circ\text{C}/\text{min}$. The sample is held at 975°C for 1 h before cooling it down to 900°C at
277 $1^\circ\text{C}/\text{min}$ and held for 1 h. Finally, the sample is allowed to furnace-cool down to the room
278 temperature. The source of the Fe powders seems to have significant effect on the optimum
279 Fe:As starting stoichiometry. As powders were obtained by grinding As chunks (Alfa Aesar,
280 2-8mm, 99.9999% (metals basis)) using a mortar and pestle. Fig. ?? shows the impurity
281 percentage as a function of Fe:As stoichiometry for Fe powders (Alfa Aesar, -200 mesh, 99+%\n
282 (metals basis)) with $0.74 \mu\text{m}$ in size. Phase pure Fe_2As is obtained for Fe:As ratio of 1.95:1.
283 Increasing the Fe content results in Fe impurity and decreasing Fe content results in FeAs
284 impurity.

285 While using the 200 mesh size Fe powders yielded pure Fe_2As , the residual resistivity ratio
286 from the transport measurements indicated Fe_2As to be a bad metal. In an attempt to reduce
287 the presence of trace impurities, more pure Fe powders were sourced. Fe powders (Alfa
288 Aesar, $10 \mu\text{m}$, spherical, >99.99% (metals basis)) with $10 \mu\text{m}$ in size were used for preparing
289 batches of 1 g of Fe_2As crystals. In order to reduce processing errors, before vacuum sealing

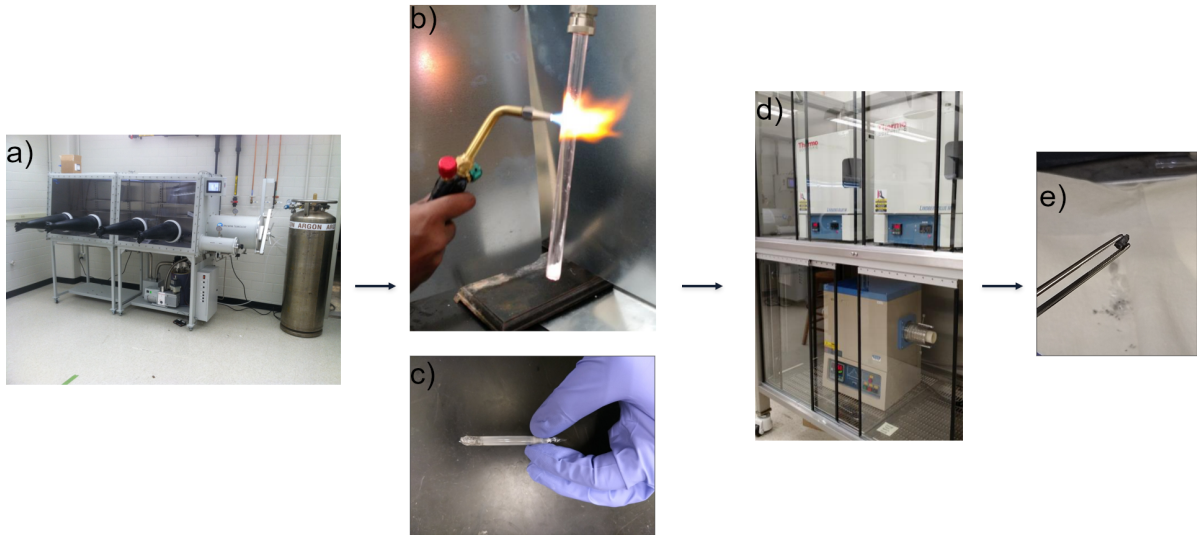


Figure 3.1: The process of making bulk materials using traditional solid state synthesis technique is shown here. The powders mixed inside the glovebox in (a) are transferred to a quartz tube and vacuum sealed in (b). The vacuum sealed ampoule in (c) is placed inside the box furnace in (d) and subjected to a heating profile. (e) shows the final ingot obtained in case of CuMnAs sample.

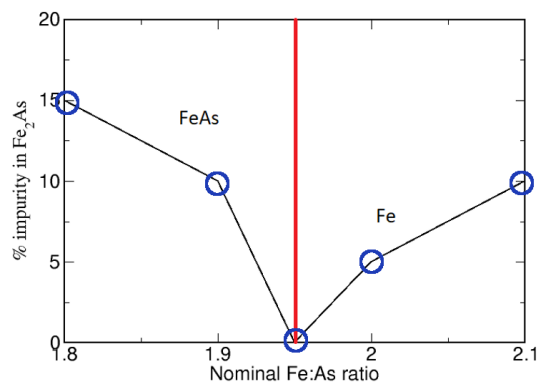


Figure 3.2: Impurity percentage as a function of Fe:As starting stoichiometry ratio with 200 mesh size Fe powders for making Fe₂As samples.

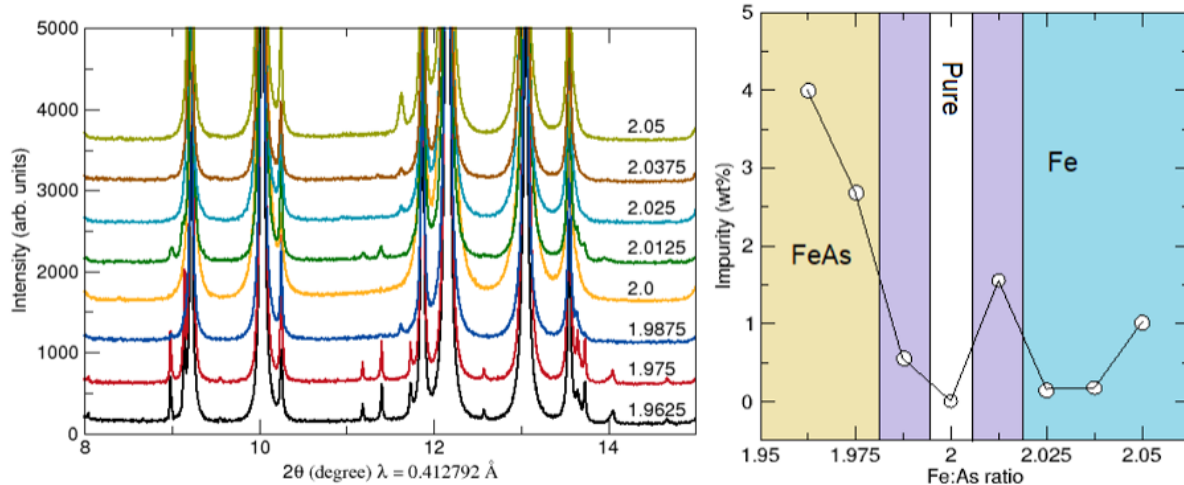


Figure 3.3: Synchrotron x-ray diffraction data of Fe_2As for different ratios of Fe:As from 10 μm Fe powders is shown in (a) and the corresponding impurity percentage is shown in (b).

290 the quartz tube, a magnet was moved from top to bottom of the outer walls of the tube in a
 291 rocking fashion to remove any Fe powders sticking to the inner walls of the tube. Finally, the
 292 synthesized Fe_2As crystals were crushed into powders and sent to the 11-BM beamline at the
 293 Advanced Photon Source in Argonne National Laboratory for synchrotron x-ray diffraction
 294 measurements. The results of the 8 samples with different Fe:As ratio is shown in Fig. 3.3(a).
 295 The results from this data suggest that Fe:As ratio of 2:1 which is also the stoichiometric ratio,
 296 is optimum to produce phase pure samples as shown in Fig. 3.3(b). Similar to earlier results,
 297 increasing the Fe:As ratio above 2 precipitates out Fe impurity and decreasing the Fe:As ratio
 298 results in FeAs impurity. The region colored in purple in Fig. 3.3(b) contained the opposite of
 299 the expected impurity. The purple region on the excess Fe side contained FeAs impurity and
 300 on the lower Fe side contained Fe impurity. I attribute this inconsistency to random errors.

301 3.2 Synthesis of compounds in the Cu-Mn-As system

302 Compounds in the Cu-Mn-As system powders are synthesized by mixing Cu powders (Alfa
 303 Aesar, -100+325 mesh, spherical, 99.9% (metals basis)), Mn powders ground from Mn chips
 304 (99.98% (metals basis)) and As powders ground from chunks (Alfa Aesar, 2-8mm, 99.9999%
 305 (metals basis)) inside the Ar atmosphere and following the same heating procedure as in
 306 the case of Fe_2As . To synthesize binary compounds Mn_2As and Mn_3As_2 , excess Mn has
 307 to be added into the mixture. Mn:As ratio of 2.1:1 and 3.1:2 is required to synthesize pure
 308 phase Mn_2As and Mn_3As_2 , respectively. In case of Mn_2As , when Mn and As powders are
 309 mixed in stoichiometric ratio, Mn_3As_2 impurity is formed due to peritectic reaction [41].

310 The ratio of Cu:Mn:As powders determines the final product. When Cu:Mn:As ratio is
311 0.82:1.18:1, the hexagonal polymorph of CuMnAs is stabilized. From literature, when Cu,
312 Mn and As powders are mixed in equal proportions, orthorhombic CuMnAs is formed.
313 However, in our synthesis procedure, we observe a mixture of tetragonal and orthorhombic
314 CuMnAs. The difference in the final product comes from the use of an Alumina crucible
315 inside the quartz tube. I have synthesized tetragonal CuMnAs by substituting equal amounts
316 of Mn with Cu powders. An almost stoichiometric tetragonal CuMnAs has been reported
317 in literature by substituting small amounts of Mn with As [42]. I also synthesized the near
318 stoichiometric tetragonal CuMnAs by replicating the procedure from literature including
319 the use of Alumina crucible. The heating procedure has a significant impact on the quality
320 of the tetragonal CuMnAs crystals. Tetragonal CuMnAs undergoes a phase transition at
321 around 800°C which makes it difficult to synthesize large crystals using traditional solid state
322 synthesis routes. Out of the three elemental powders, Cu is the element that is being directly
323 used in the powder form. Hence, it is prone to oxidation easily. However, Cu powders can
324 be easily reduced using H₂ gas flow reaction by heating it to 600°C for holding it for 6 hours.

325 3.3 Materials characterization

326 3.3.1 X-ray diffraction

327 Powder x-ray diffraction measurements were carried out primarily at the Bruker D8 Advance
328 powder x-ray diffractometer with Mo source using the capillary stage. Since the materials
329 used here contain As and other transition metal atoms which absorb x-rays significantly,
330 thin capillaries of 0.43 mm in diameter were used. In addition to that, the powders were
331 diluted with appropriate amounts of amorphous silica to account for x-ray absorption. Most
332 x-ray measurements on CuMnAs samples were carried out on the Bruker D8 Advance x-ray
333 diffraction with Cu source using a reflective stage. In these measurements, the samples were
334 not diluted with silica since absorption is not an issue. However, significant sample texturing
335 was observed which has to be taken into account while carrying out Rietveld refinement.
336 Certain samples were also measured at the 11-BM beamline of the Advanced Photon Source
337 in Argonne National Laboratory. The powders were mounted onto 0.7 mm diameter quartz
338 capillaries and vacuum sealed before fitting it inside a Kapton capillary for measurement.
339 The high energy synchrotron beam wavelength that was used at 11-BM beamline corresponds
340 to 0.4128 Å. Rietveld refinement of the powder x-ray diffraction data was carried out using
341 TOPAS and GSAS-II [43, 44].

342 Hexagonal Cu_{0.82}Mn_{1.18}As crystals were sent to SCS X-ray facility for single crystal x-ray
343 diffraction measurement on a Bruker X8 Apex II diffractometer. Tiny single crystals of the
344 size of around 100 μm were fractured out from a large ingot and used for the measurement.
345 Alignment of large single crystals of Fe₂As and Cu_{0.82}Mn_{1.18}As for the purpose of aligned

346 SQUID magnetometry, magnetotransport and inelastic neutron scattering measurements
347 were carried out using a Laue System with a Multiwire 2D Detector at both MRL x-ray
348 laboratory as well as at Spallation Neutron Source. The Laue diffractometer was only used
349 to align samples from the symmetry of the Laue pattern. Indexing of the patterns were not
350 carried out using the Northstar software due to issues with the software. The out-of-plane
351 alignment in Cu_{0.82}Mn_{1.18}As single crystal was also confirmed using the reflective stage of
352 Bruker D8 Advance diffractometer with Mo source.

353 **3.3.2 Calorimetry**

354 Thermogravimetric analysis (TGA) is a thermal analysis technique where the mass of the
355 sample is tracked over a range of temperatures. It is particularly useful for detecting changes
356 such as sublimation or evaporation of a phase or any kind of absorption/desorption processes.
357 Powders or crystals of around 10 mg can be loaded onto an Alumina cup and heated up to
358 1000°C for TGA. All the samples were measured in the Q50 TGA instrument upto above
359 400°C under N₂ atmosphere to check if the sample loses its integrity at this temperature range
360 or not. No transitions were observed in any of the samples measured and further analysis
361 was carried out using differential scanning calorimetry (DSC). This measurement technique,
362 although not very useful in this case, is necessary to prevent any accidental coating of the
363 inner chamber during DSC measurements.

364 DSC is a calorimetry technique where the difference in the heat required to keep the sample
365 at the same temperature as the reference is recorded as a function of temperature. It is a
366 sensitive measurement technique and is useful for detecting magnetic transitions such as the
367 Néel temperature or any spin canting transition. DSC measurements for all samples were
368 carried out in the DSC2500 instrument. The sample powders, weighing between 4 mg to
369 8 mg, were loaded onto Alumina pans and subjected to heat-cool-heat cycles between -180°C
370 and 400° at 10°C/min.

371 Differential thermal analysis (DTA) is similar to DSC except that the temperature difference
372 between the sample and reference is recorded for identical thermal cycles. DTA measure-
373 ments were carried out on a Shimadzu DTA-50 up to 1200°C in some samples at a heating
374 rate of 20°C/min under N₂ atmosphere. The advantage of using DTA is that it can go up
375 to very high temperatures which is useful for detecting melting point and any other phase
376 transition that is beyond the range of DSC. The presence of As in the samples makes it im-
377 possible to use the standard DTA Alumina cups for measurement. To prevent contamination
378 of the room with As vapors, special quartz ampoules were designed and commissioned from
379 the SCS Glass shop. The ampoules were made by cutting 3 mm and 4 mm OD quartz tubes
380 in 85 mm lengths and creating a flat-bottom bulb of 5 mm diameter at one end of the tube as
381 shown in Fig. 3.4(a). About 20 mg to 40 mg of sample powders were vacuum sealed in the
382 quartz ampoules and similar amount of Alumina powder was sealed as reference as shown

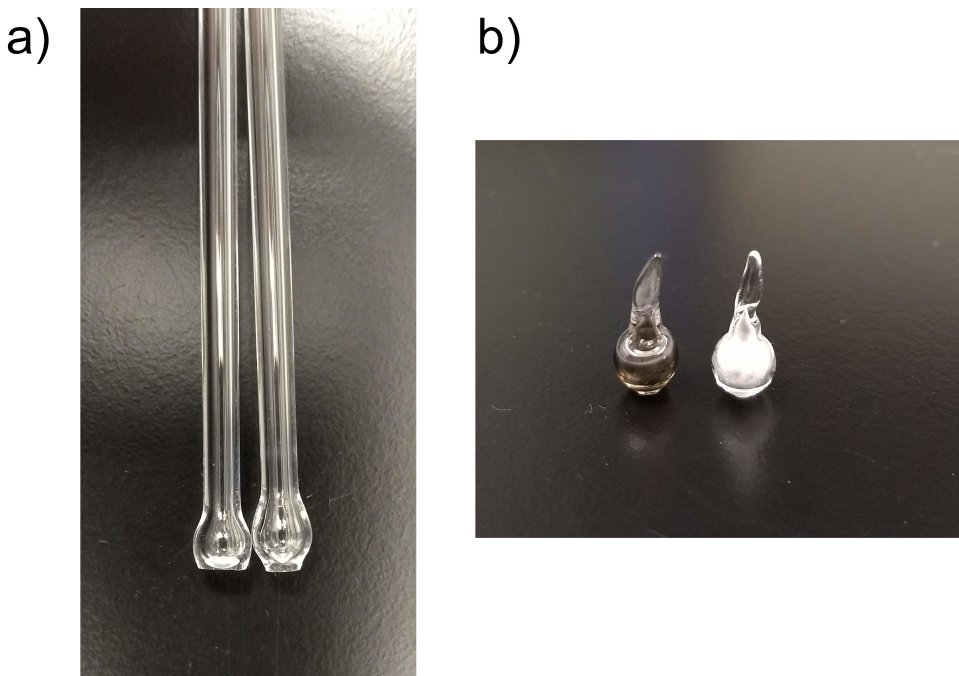


Figure 3.4: The flat-bottom bulk of the quartz ampoules is shown in (a) and (b) shows the final powder-containing vacuum sealed ampoules.

383 in Fig. 3.4(b). The use of quartz ampoules, however, prevents detection of subtle transitions
384 such as magnetic transitions. Hence, DTA can be used in conjunction with DSC to identify
385 all transition temperatures.

386 3.3.3 SQUID magnetometry

387 SQUID measurements for all the samples were carried out in a Quantum Design MPMS3
388 (Magnetic Property Measurement System) in the DC mode. The DC moment was tracked
389 as a function of applied field as well as temperature. In magnetic hysteresis measurements,
390 fields up to 10 kOe were applied across six quadrants to account for the initial magnetization
391 curve. Field cooling measurements refer to the application of magnetic field at 400°C followed
392 by cooling of the sample. Zero field cooling measurements are carried out by first cooling
393 the sample in the absence of a field, followed by the application of an external field and
394 then, heating the sample. The sample moment is measured at certain intervals across the
395 temperature range. The SQUID measurements have been carried out for the powders of
396 Fe₂As, Cu_{0.82}Mn_{1.18}As, tetragonal CuMnAs and Mn₃As₂, and the single crystals of Fe₂As
397 and Cu_{0.82}Mn_{1.18}As. In case of powders, 20 mg to 40 mg of powders were filled into a VSM
398 powder sample holder inside the Ar atmosphere glovebox. This capillary was snapped onto
399 a MPMS3 brass half tube sample holder and wrapped with a small amount of insulating tape
400 to keep it fixed. For single crystal measurements, aligned samples were fixed on the MPMS3

401 Quartz Paddle Sample Holder using GE Varnish and later removed using ethanol.

402 **3.3.4 Transport measurements**

403 **3.4 Neutron scattering**

404 **3.4.1 Neutron powder diffraction**

405 **3.4.2 Inelastic neutron scattering**

Chapter 4

Magnetic structure refinement from neutron diffraction measurements

406 Lorem ipsum dolor sit amet, consectetur adipiscing elit. Etiam lobortis facilisis sem. Nullam
407 nec mi et neque pharetra sollicitudin. Praesent imperdiet mi nec ante. Donec ullamcorper,
408 felis non sodales commodo, lectus velit ultrices augue, a dignissim nibh lectus placerat pede.
409 Vivamus nunc nunc, molestie ut, ultricies vel, semper in, velit. Ut porttitor. Praesent in sapien.
410 Lorem ipsum dolor sit amet, consectetur adipiscing elit. Duis fringilla tristique neque. Sed
411 interdum libero ut metus. Pellentesque placerat. Nam rutrum augue a leo. Morbi sed elit sit
412 amet ante lobortis sollicitudin. Praesent blandit blandit mauris. Praesent lectus tellus, aliquet
413 aliquam, luctus a, egestas a, turpis. Mauris lacinia lorem sit amet ipsum. Nunc quis urna
414 dictum turpis accumsan semper.

415 Lorem ipsum dolor sit amet, consectetur adipiscing elit. Etiam lobortis facilisis sem.
416 Nullam nec mi et neque pharetra sollicitudin. Praesent imperdiet mi nec ante. Donec
417 ullamcorper, felis non sodales commodo, lectus velit ultrices augue, a dignissim nibh lectus
418 placerat pede. Vivamus nunc nunc, molestie ut, ultricies vel, semper in, velit. Ut porttitor.
419 Praesent in sapien. Lorem ipsum dolor sit amet, consectetur adipiscing elit. Duis fringilla
420 tristique neque. Sed interdum libero ut metus. Pellentesque placerat. Nam rutrum augue
421 a leo. Morbi sed elit sit amet ante lobortis sollicitudin. Praesent blandit blandit mauris.
422 Praesent lectus tellus, aliquet aliquam, luctus a, egestas a, turpis. Mauris lacinia lorem sit
423 amet ipsum. Nunc quis urna dictum turpis accumsan semper.

424 Lorem ipsum dolor sit amet, consectetur adipiscing elit. Etiam lobortis facilisis sem.
425 Nullam nec mi et neque pharetra sollicitudin. Praesent imperdiet mi nec ante. Donec
426 ullamcorper, felis non sodales commodo, lectus velit ultrices augue, a dignissim nibh lectus
427 placerat pede. Vivamus nunc nunc, molestie ut, ultricies vel, semper in, velit. Ut porttitor.
428 Praesent in sapien. Lorem ipsum dolor sit amet, consectetur adipiscing elit. Duis fringilla
429 tristique neque. Sed interdum libero ut metus. Pellentesque placerat. Nam rutrum augue
430 a leo. Morbi sed elit sit amet ante lobortis sollicitudin. Praesent blandit blandit mauris.
431 Praesent lectus tellus, aliquet aliquam, luctus a, egestas a, turpis. Mauris lacinia lorem sit
432 amet ipsum. Nunc quis urna dictum turpis accumsan semper.

433 Lorem ipsum dolor sit amet, consectetur adipiscing elit. Etiam lobortis facilisis sem.
434 Nullam nec mi et neque pharetra sollicitudin. Praesent imperdiet mi nec ante. Donec
435 ullamcorper, felis non sodales commodo, lectus velit ultrices augue, a dignissim nibh lectus

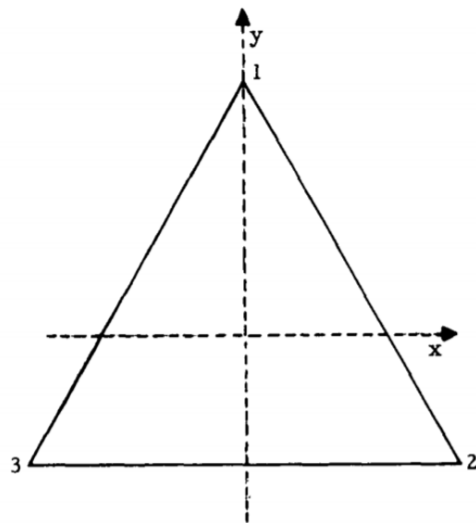


Figure 4.1: Electronic band structure

	E	C_3	C_3^2	σ_1	σ_2	σ_3
E	E	C_3	C_3^2	σ_1	σ_2	σ_3
C_3	C_3	C_3^2	E	σ_3	σ_1	σ_2
C_3^2	C_3^2	E	C_3	σ_2	σ_3	σ_1
σ_1	σ_1	σ_2	σ_3	E	C_3	C_3^2
σ_2	σ_2	σ_3	σ_1	C_3^2	E	C_3
σ_3	σ_3	σ_1	σ_2	C_3	C_3^2	E

Figure 4.2: Electronic band structure

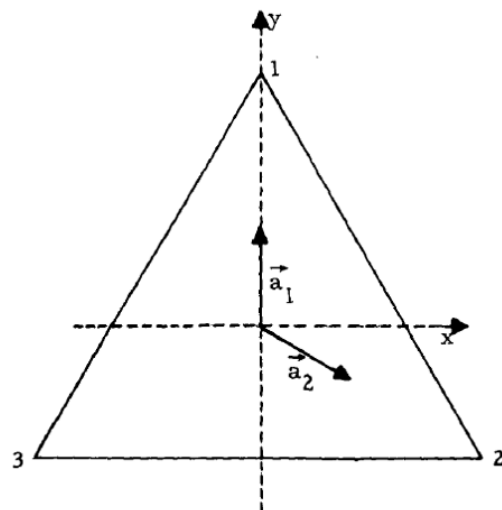


Figure 4.3: Electronic band structure

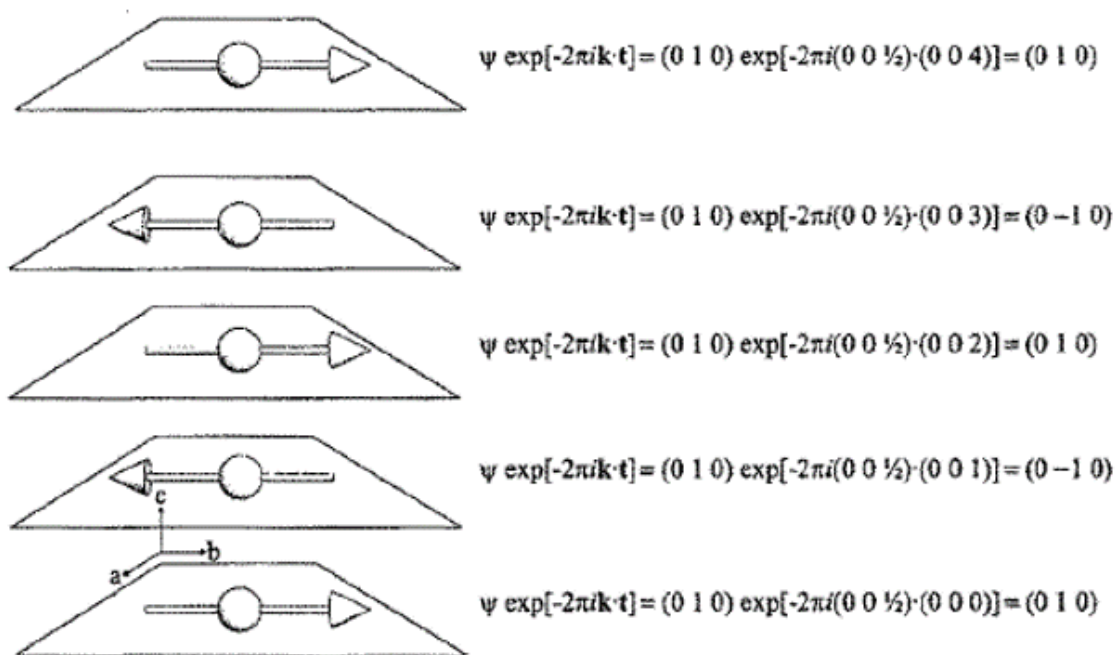


Figure 4.4: Electronic band structure

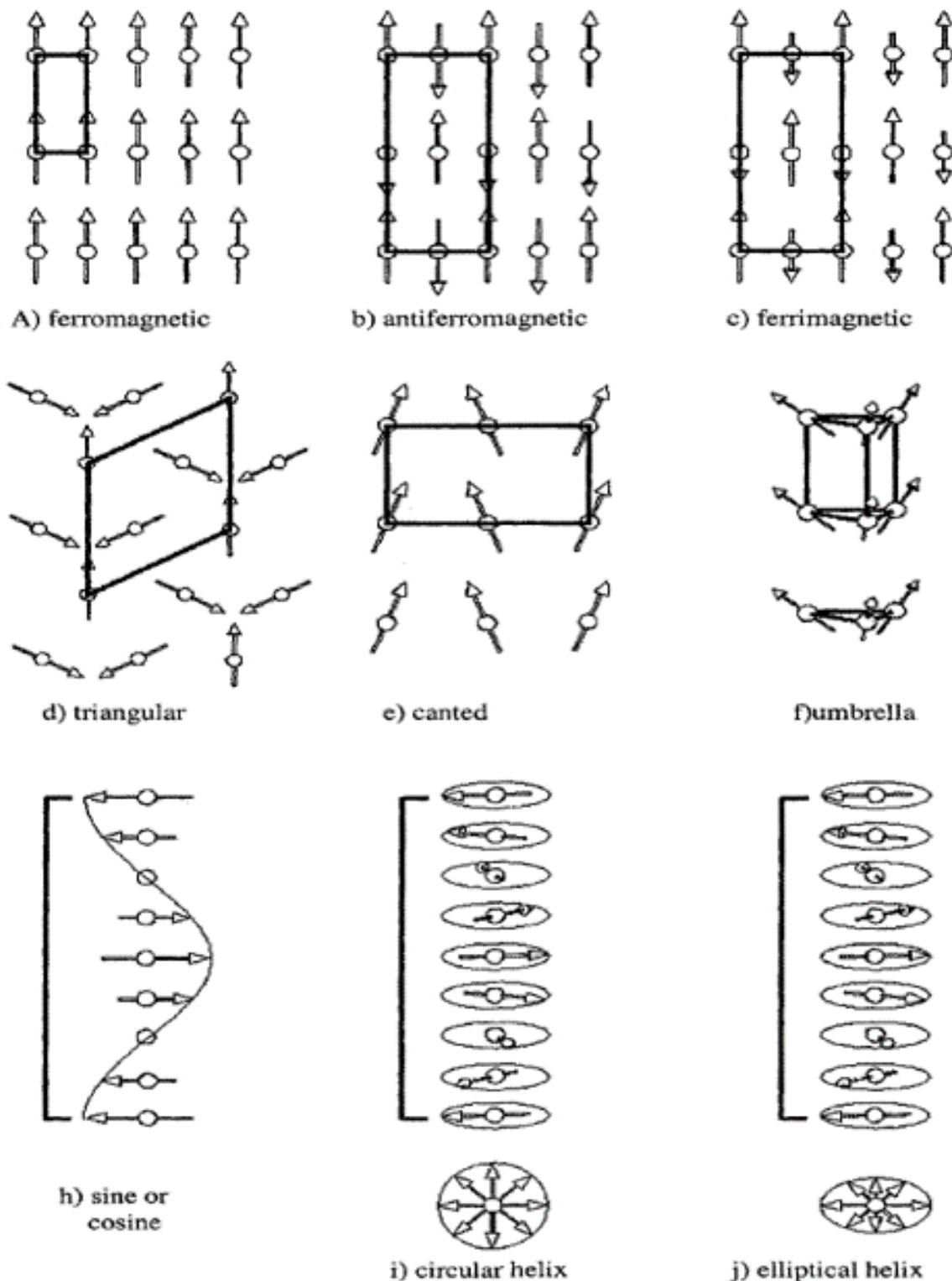


Figure 4.5: Electronic band structure

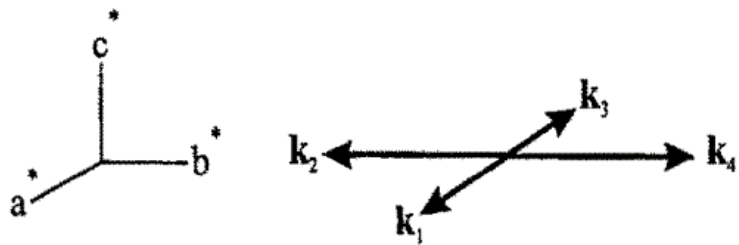


Figure 4.6: Electronic band structure

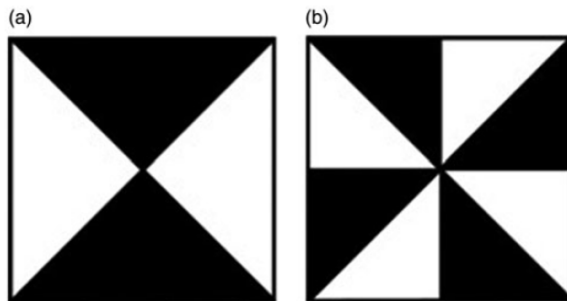


Figure 4.7: Electronic band structure

436 placerat pede. Vivamus nunc nunc, molestie ut, ultricies vel, semper in, velit. Ut porttitor.
437 Praesent in sapien. Lorem ipsum dolor sit amet, consectetuer adipiscing elit. Duis fringilla
438 tristique neque. Sed interdum libero ut metus. Pellentesque placerat. Nam rutrum augue
439 a leo. Morbi sed elit sit amet ante lobortis sollicitudin. Praesent blandit blandit mauris.
440 Praesent lectus tellus, aliquet aliquam, luctus a, egestas a, turpis. Mauris lacinia lorem sit
441 amet ipsum. Nunc quis urna dictum turpis accumsan semper.
442 Lorem ipsum dolor sit amet, consectetuer adipiscing elit. Etiam lobortis facilisis sem.
443 Nullam nec mi et neque pharetra sollicitudin. Praesent imperdiet mi nec ante. Donec
444 ullamcorper, felis non sodales commodo, lectus velit ultrices augue, a dignissim nibh lectus
445 placerat pede. Vivamus nunc nunc, molestie ut, ultricies vel, semper in, velit. Ut porttitor.
446 Praesent in sapien. Lorem ipsum dolor sit amet, consectetuer adipiscing elit. Duis fringilla
447 tristique neque. Sed interdum libero ut metus. Pellentesque placerat. Nam rutrum augue
448 a leo. Morbi sed elit sit amet ante lobortis sollicitudin. Praesent blandit blandit mauris.
449 Praesent lectus tellus, aliquet aliquam, luctus a, egestas a, turpis. Mauris lacinia lorem sit
450 amet ipsum. Nunc quis urna dictum turpis accumsan semper.
451 Lorem ipsum dolor sit amet, consectetuer adipiscing elit. Etiam lobortis facilisis sem.
452 Nullam nec mi et neque pharetra sollicitudin. Praesent imperdiet mi nec ante. Donec
453 ullamcorper, felis non sodales commodo, lectus velit ultrices augue, a dignissim nibh lectus
454 placerat pede. Vivamus nunc nunc, molestie ut, ultricies vel, semper in, velit. Ut porttitor.

455 Praesent in sapien. Lorem ipsum dolor sit amet, consectetuer adipiscing elit. Duis fringilla
456 tristique neque. Sed interdum libero ut metus. Pellentesque placerat. Nam rutrum augue
457 a leo. Morbi sed elit sit amet ante lobortis sollicitudin. Praesent blandit blandit mauris.
458 Praesent lectus tellus, aliquet aliquam, luctus a, egestas a, turpis. Mauris lacinia lorem sit
459 amet ipsum. Nunc quis urna dictum turpis accumsan semper.

Chapter 5

Discovery and magnetic frustration of hexagonal Cu_{0.82}Mn_{1.18}As

460 Lorem ipsum dolor sit amet, consectetur adipiscing elit. Etiam lobortis facilisis sem. Nullam
461 nec mi et neque pharetra sollicitudin. Praesent imperdiet mi nec ante. Donec ullamcorper,
462 felis non sodales commodo, lectus velit ultrices augue, a dignissim nibh lectus placerat pede.
463 Vivamus nunc nunc, molestie ut, ultricies vel, semper in, velit. Ut porttitor. Praesent in sapien.
464 Lorem ipsum dolor sit amet, consectetur adipiscing elit. Duis fringilla tristique neque. Sed
465 interdum libero ut metus. Pellentesque placerat. Nam rutrum augue a leo. Morbi sed elit sit
466 amet ante lobortis sollicitudin. Praesent blandit blandit mauris. Praesent lectus tellus, aliquet
467 aliquam, luctus a, egestas a, turpis. Mauris lacinia lorem sit amet ipsum. Nunc quis urna
468 dictum turpis accumsan semper.

469 Lorem ipsum dolor sit amet, consectetur adipiscing elit. Etiam lobortis facilisis sem.
470 Nullam nec mi et neque pharetra sollicitudin. Praesent imperdiet mi nec ante. Donec
471 ullamcorper, felis non sodales commodo, lectus velit ultrices augue, a dignissim nibh lectus
472 placerat pede. Vivamus nunc nunc, molestie ut, ultricies vel, semper in, velit. Ut porttitor.
473 Praesent in sapien. Lorem ipsum dolor sit amet, consectetur adipiscing elit. Duis fringilla
474 tristique neque. Sed interdum libero ut metus. Pellentesque placerat. Nam rutrum augue
475 a leo. Morbi sed elit sit amet ante lobortis sollicitudin. Praesent blandit blandit mauris.
476 Praesent lectus tellus, aliquet aliquam, luctus a, egestas a, turpis. Mauris lacinia lorem sit
477 amet ipsum. Nunc quis urna dictum turpis accumsan semper.

478 Lorem ipsum dolor sit amet, consectetur adipiscing elit. Etiam lobortis facilisis sem.
479 Nullam nec mi et neque pharetra sollicitudin. Praesent imperdiet mi nec ante. Donec
480 ullamcorper, felis non sodales commodo, lectus velit ultrices augue, a dignissim nibh lectus
481 placerat pede. Vivamus nunc nunc, molestie ut, ultricies vel, semper in, velit. Ut porttitor.
482 Praesent in sapien. Lorem ipsum dolor sit amet, consectetur adipiscing elit. Duis fringilla
483 tristique neque. Sed interdum libero ut metus. Pellentesque placerat. Nam rutrum augue
484 a leo. Morbi sed elit sit amet ante lobortis sollicitudin. Praesent blandit blandit mauris.
485 Praesent lectus tellus, aliquet aliquam, luctus a, egestas a, turpis. Mauris lacinia lorem sit
486 amet ipsum. Nunc quis urna dictum turpis accumsan semper.

487 Lorem ipsum dolor sit amet, consectetur adipiscing elit. Etiam lobortis facilisis sem.
488 Nullam nec mi et neque pharetra sollicitudin. Praesent imperdiet mi nec ante. Donec
489 ullamcorper, felis non sodales commodo, lectus velit ultrices augue, a dignissim nibh lectus

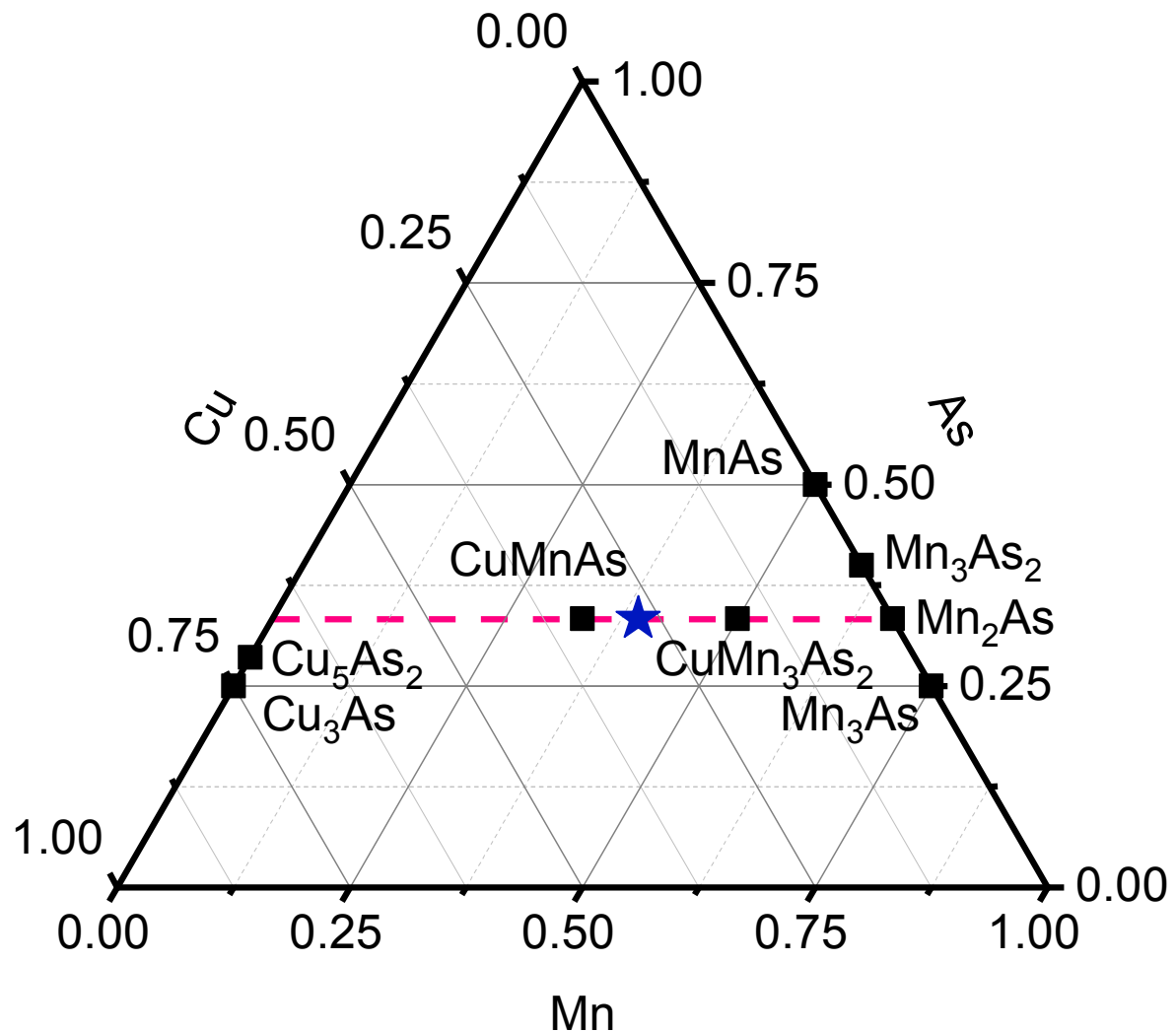


Figure 5.1: Electronic band structure

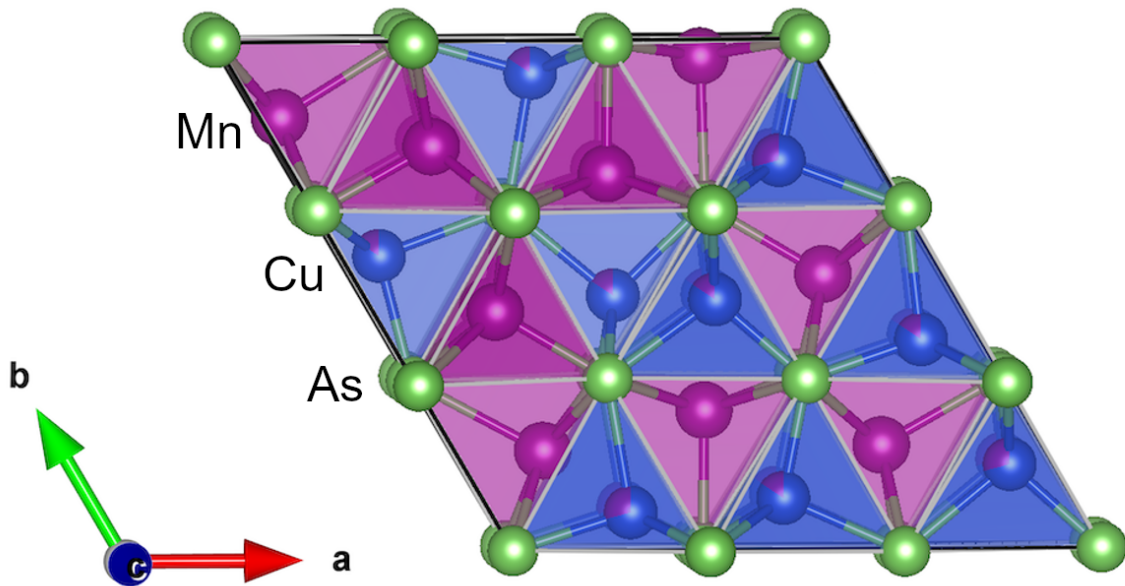


Figure 5.2: Electronic band structure

490 placerat pede. Vivamus nunc nunc, molestie ut, ultricies vel, semper in, velit. Ut porttitor.
491 Praesent in sapien. Lorem ipsum dolor sit amet, consectetuer adipiscing elit. Duis fringilla
492 tristique neque. Sed interdum libero ut metus. Pellentesque placerat. Nam rutrum augue
493 a leo. Morbi sed elit sit amet ante lobortis sollicitudin. Praesent blandit blandit mauris.
494 Praesent lectus tellus, aliquet aliquam, luctus a, egestas a, turpis. Mauris lacinia lorem sit
495 amet ipsum. Nunc quis urna dictum turpis accumsan semper.
496 Lorem ipsum dolor sit amet, consectetuer adipiscing elit. Etiam lobortis facilisis sem.
497 Nullam nec mi et neque pharetra sollicitudin. Praesent imperdiet mi nec ante. Donec
498 ullamcorper, felis non sodales commodo, lectus velit ultrices augue, a dignissim nibh lectus
499 placerat pede. Vivamus nunc nunc, molestie ut, ultricies vel, semper in, velit. Ut porttitor.
500 Praesent in sapien. Lorem ipsum dolor sit amet, consectetuer adipiscing elit. Duis fringilla
501 tristique neque. Sed interdum libero ut metus. Pellentesque placerat. Nam rutrum augue
502 a leo. Morbi sed elit sit amet ante lobortis sollicitudin. Praesent blandit blandit mauris.
503 Praesent lectus tellus, aliquet aliquam, luctus a, egestas a, turpis. Mauris lacinia lorem sit
504 amet ipsum. Nunc quis urna dictum turpis accumsan semper.
505 Lorem ipsum dolor sit amet, consectetuer adipiscing elit. Etiam lobortis facilisis sem.
506 Nullam nec mi et neque pharetra sollicitudin. Praesent imperdiet mi nec ante. Donec
507 ullamcorper, felis non sodales commodo, lectus velit ultrices augue, a dignissim nibh lectus
508 placerat pede. Vivamus nunc nunc, molestie ut, ultricies vel, semper in, velit. Ut porttitor.
509 Praesent in sapien. Lorem ipsum dolor sit amet, consectetuer adipiscing elit. Duis fringilla
510 tristique neque. Sed interdum libero ut metus. Pellentesque placerat. Nam rutrum augue

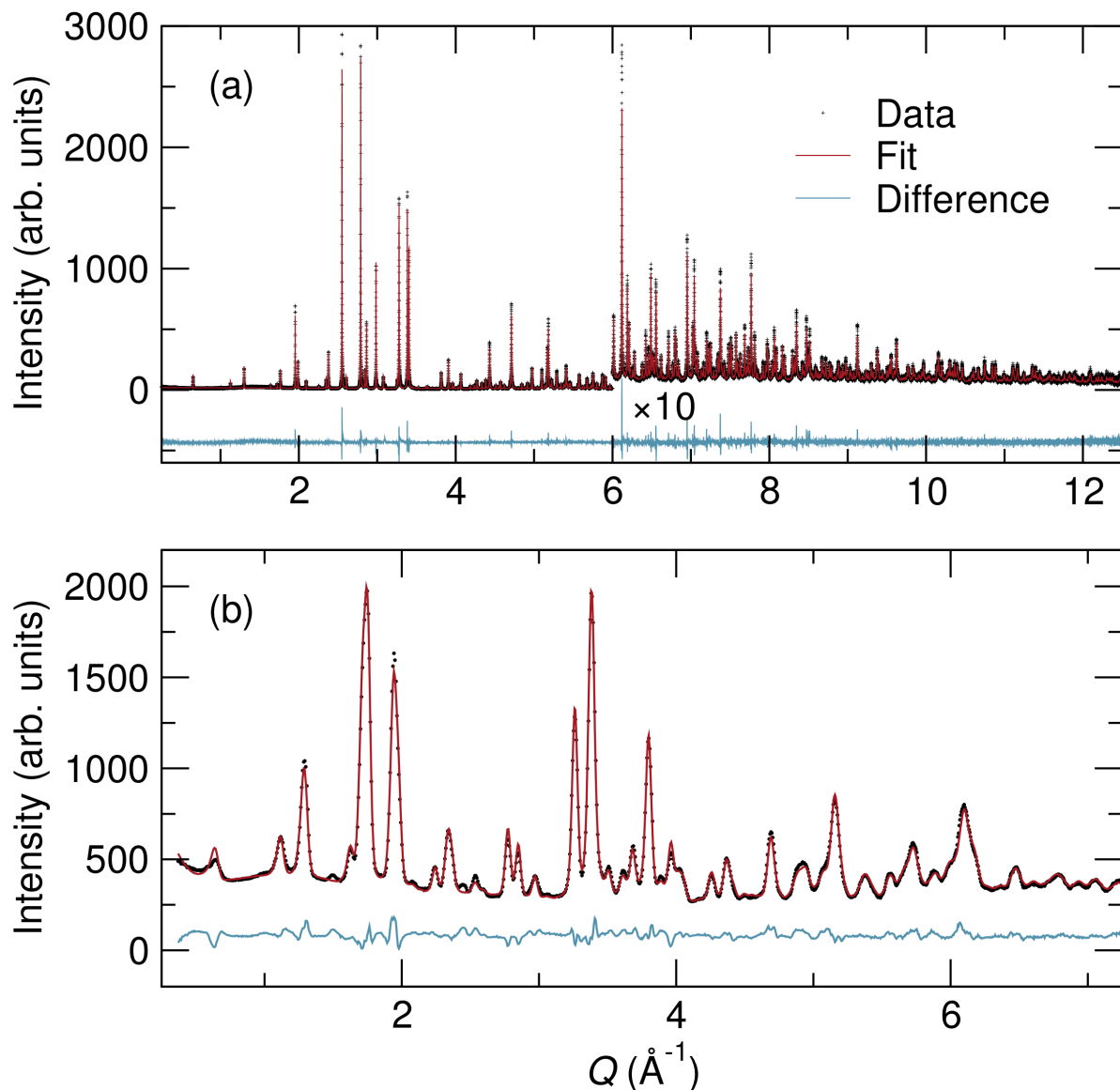


Figure 5.3: Electronic band structure

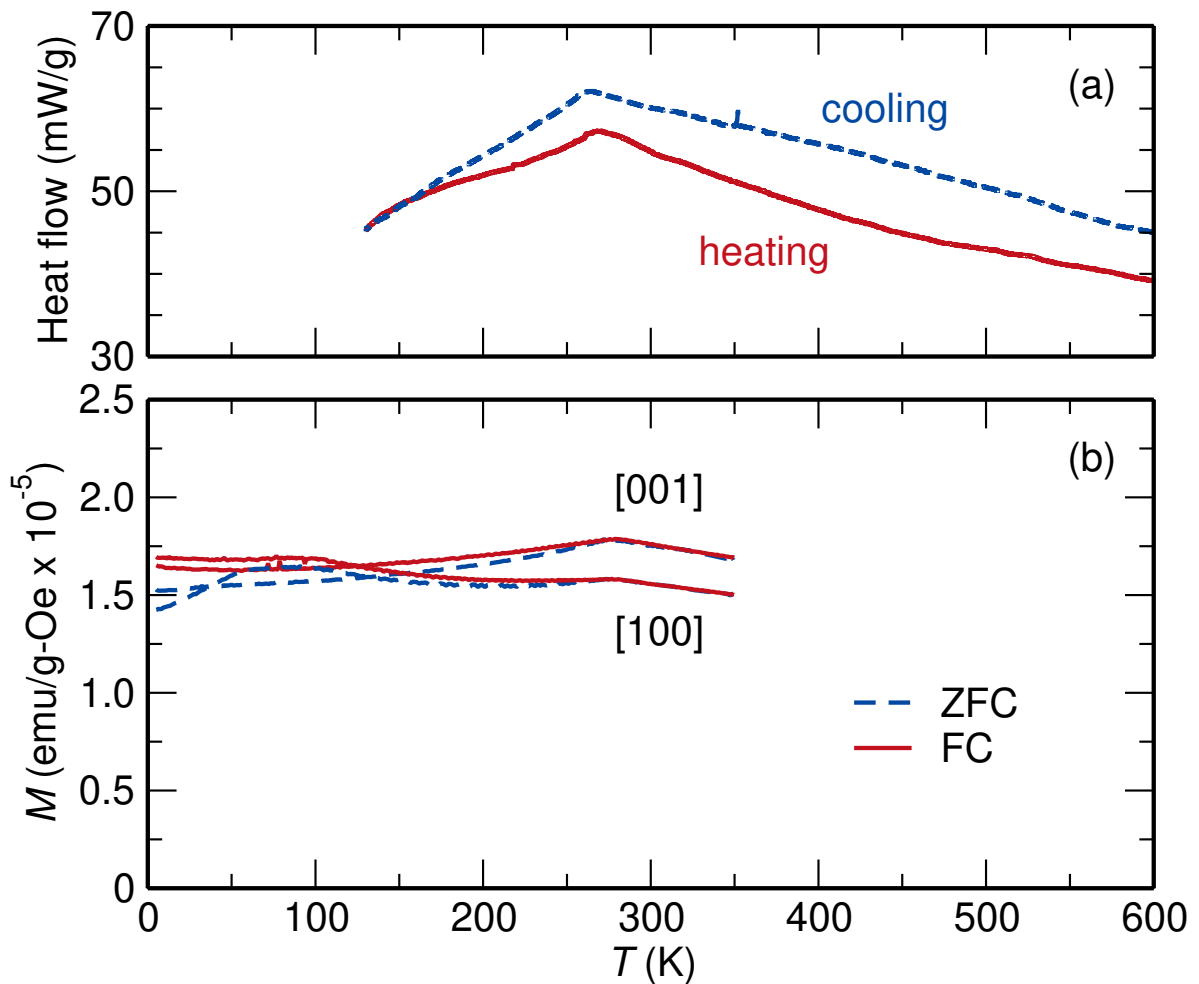


Figure 5.4: Electronic band structure

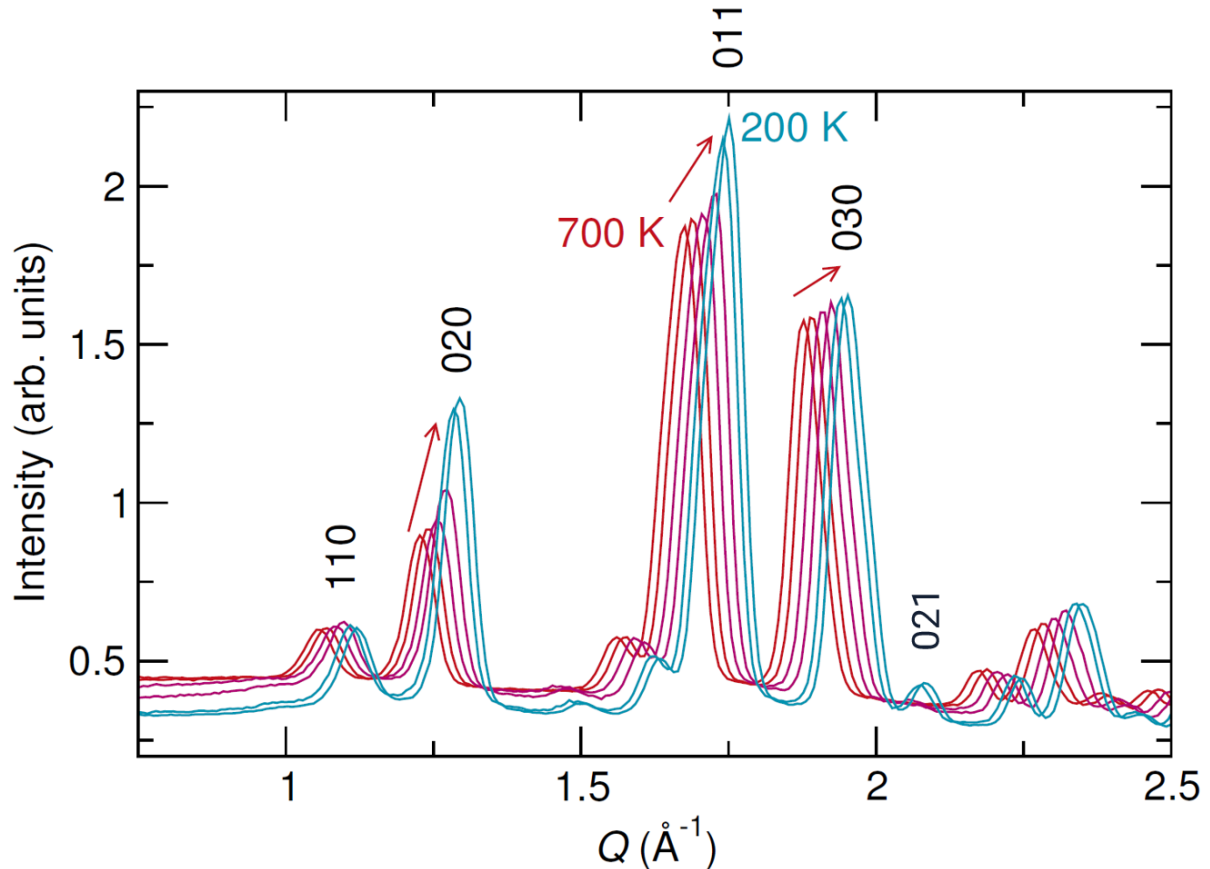


Figure 5.5: Electronic band structure

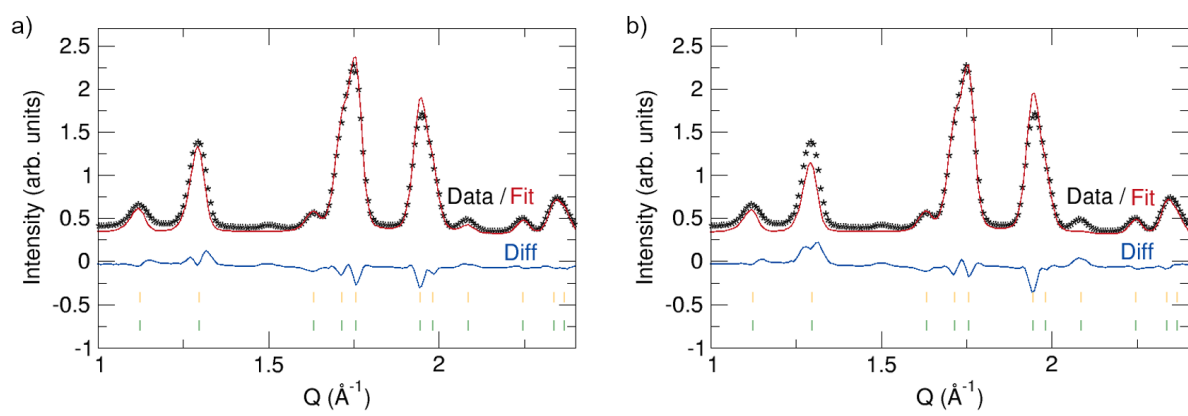


Figure 5.6: Electronic band structure

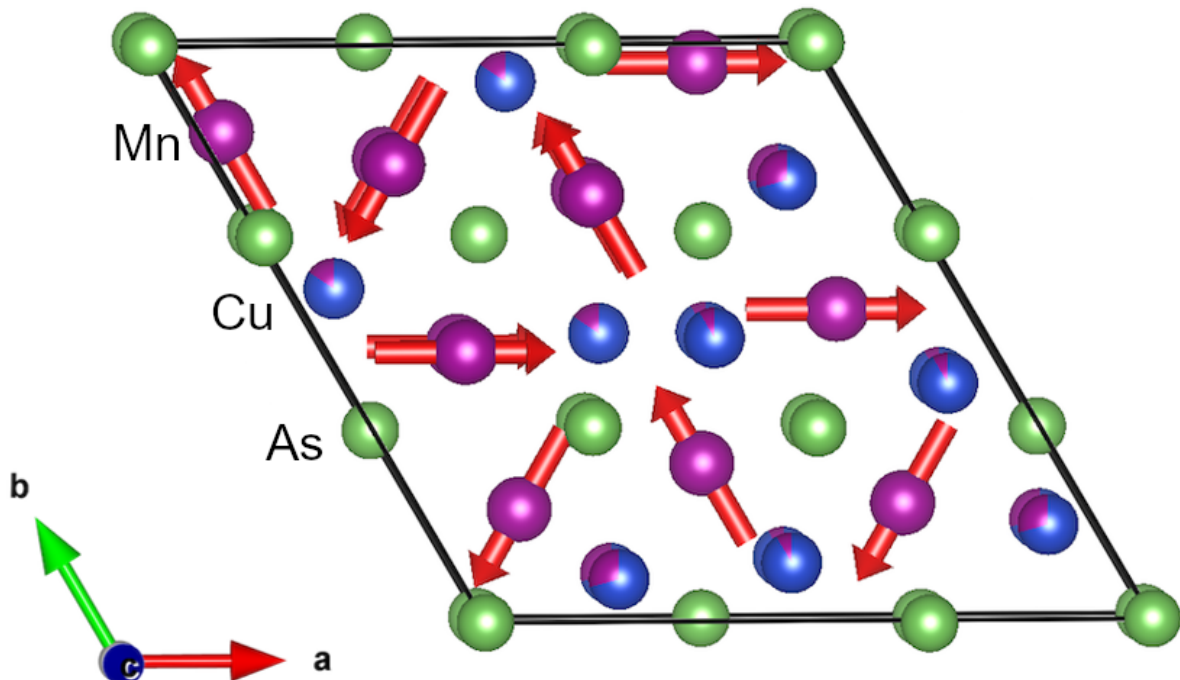


Figure 5.7: Electronic band structure

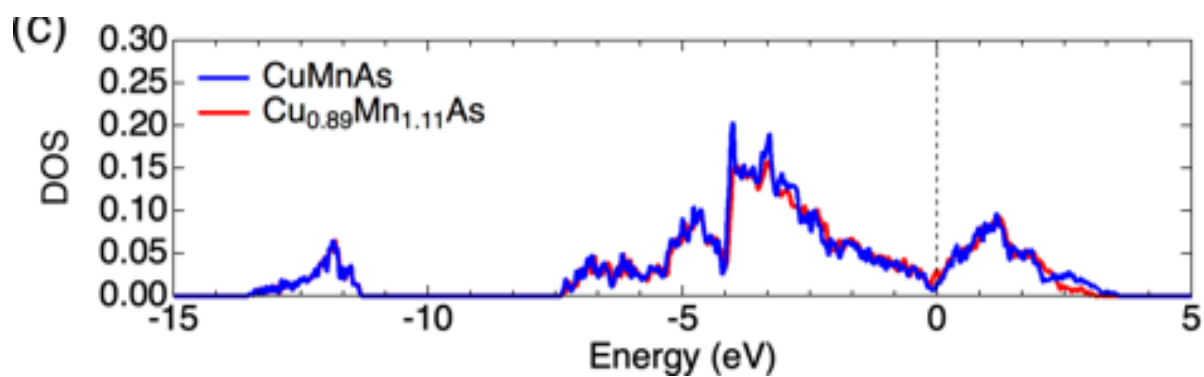


Figure 5.8: Electronic band structure

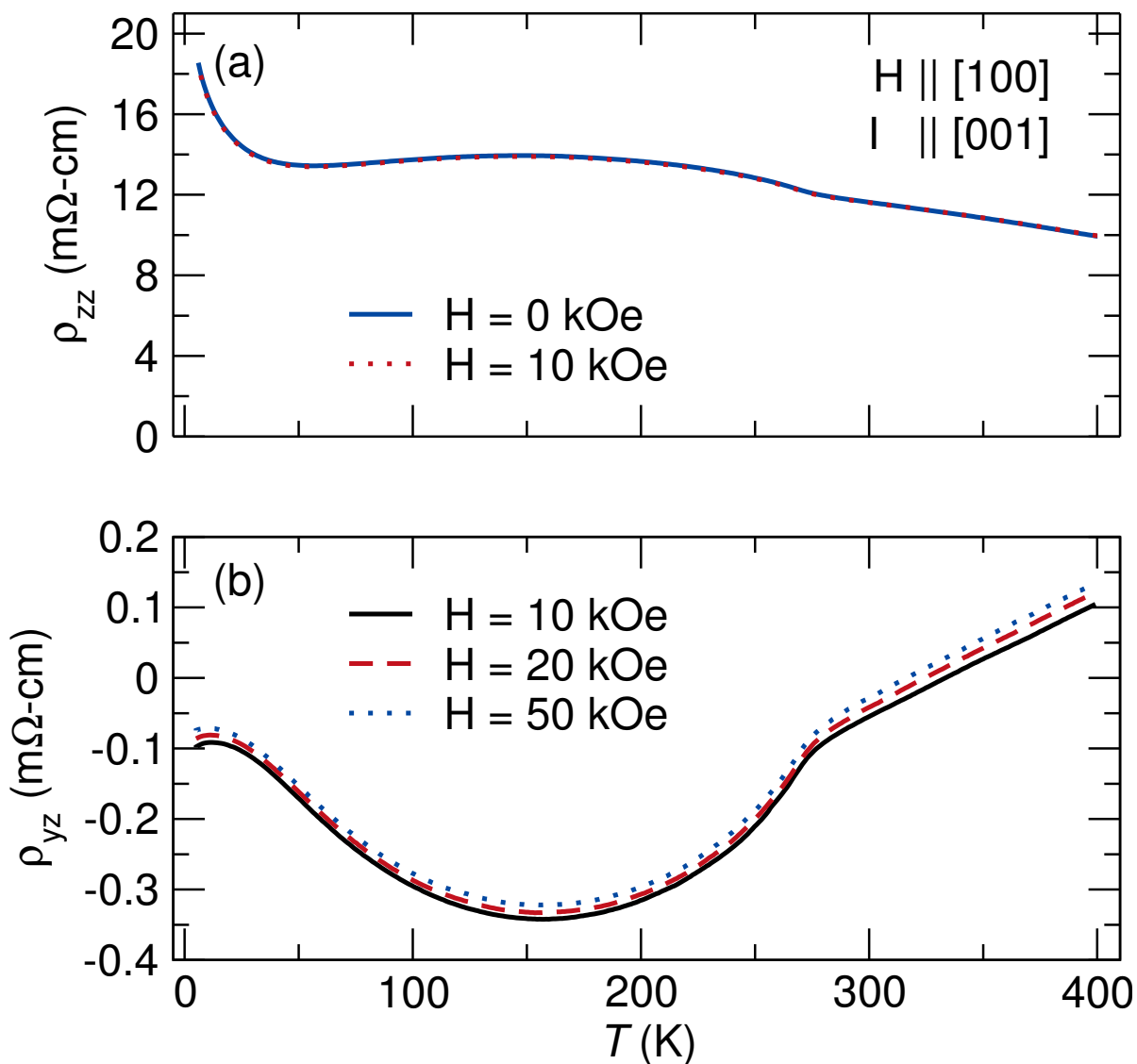


Figure 5.9: Electronic band structure

511 a leo. Morbi sed elit sit amet ante lobortis sollicitudin. Praesent blandit blandit mauris.
512 Praesent lectus tellus, aliquet aliquam, luctus a, egestas a, turpis. Mauris lacinia lorem sit
513 amet ipsum. Nunc quis urna dictum turpis accumsan semper.

Chapter 6

Two step magnetic ordering in monoclinic Mn₃As₂

514 Lorem ipsum dolor sit amet, consectetuer adipiscing elit. Etiam lobortis facilisis sem. Nullam
515 nec mi et neque pharetra sollicitudin. Praesent imperdiet mi nec ante. Donec ullamcorper,
516 felis non sodales commodo, lectus velit ultrices augue, a dignissim nibh lectus placerat pede.
517 Vivamus nunc nunc, molestie ut, ultricies vel, semper in, velit. Ut porttitor. Praesent in sapien.
518 Lorem ipsum dolor sit amet, consectetuer adipiscing elit. Duis fringilla tristique neque. Sed
519 interdum libero ut metus. Pellentesque placerat. Nam rutrum augue a leo. Morbi sed elit sit
520 amet ante lobortis sollicitudin. Praesent blandit blandit mauris. Praesent lectus tellus, aliquet
521 aliquam, luctus a, egestas a, turpis. Mauris lacinia lorem sit amet ipsum. Nunc quis urna
522 dictum turpis accumsan semper.

523 Lorem ipsum dolor sit amet, consectetuer adipiscing elit. Etiam lobortis facilisis sem.
524 Nullam nec mi et neque pharetra sollicitudin. Praesent imperdiet mi nec ante. Donec
525 ullamcorper, felis non sodales commodo, lectus velit ultrices augue, a dignissim nibh lectus
526 placerat pede. Vivamus nunc nunc, molestie ut, ultricies vel, semper in, velit. Ut porttitor.
527 Praesent in sapien. Lorem ipsum dolor sit amet, consectetuer adipiscing elit. Duis fringilla
528 tristique neque. Sed interdum libero ut metus. Pellentesque placerat. Nam rutrum augue
529 a leo. Morbi sed elit sit amet ante lobortis sollicitudin. Praesent blandit blandit mauris.
530 Praesent lectus tellus, aliquet aliquam, luctus a, egestas a, turpis. Mauris lacinia lorem sit
531 amet ipsum. Nunc quis urna dictum turpis accumsan semper.

532 Lorem ipsum dolor sit amet, consectetuer adipiscing elit. Etiam lobortis facilisis sem.
533 Nullam nec mi et neque pharetra sollicitudin. Praesent imperdiet mi nec ante. Donec
534 ullamcorper, felis non sodales commodo, lectus velit ultrices augue, a dignissim nibh lectus
535 placerat pede. Vivamus nunc nunc, molestie ut, ultricies vel, semper in, velit. Ut porttitor.
536 Praesent in sapien. Lorem ipsum dolor sit amet, consectetuer adipiscing elit. Duis fringilla
537 tristique neque. Sed interdum libero ut metus. Pellentesque placerat. Nam rutrum augue
538 a leo. Morbi sed elit sit amet ante lobortis sollicitudin. Praesent blandit blandit mauris.
539 Praesent lectus tellus, aliquet aliquam, luctus a, egestas a, turpis. Mauris lacinia lorem sit
540 amet ipsum. Nunc quis urna dictum turpis accumsan semper.

541 Lorem ipsum dolor sit amet, consectetuer adipiscing elit. Etiam lobortis facilisis sem.
542 Nullam nec mi et neque pharetra sollicitudin. Praesent imperdiet mi nec ante. Donec
543 ullamcorper, felis non sodales commodo, lectus velit ultrices augue, a dignissim nibh lectus

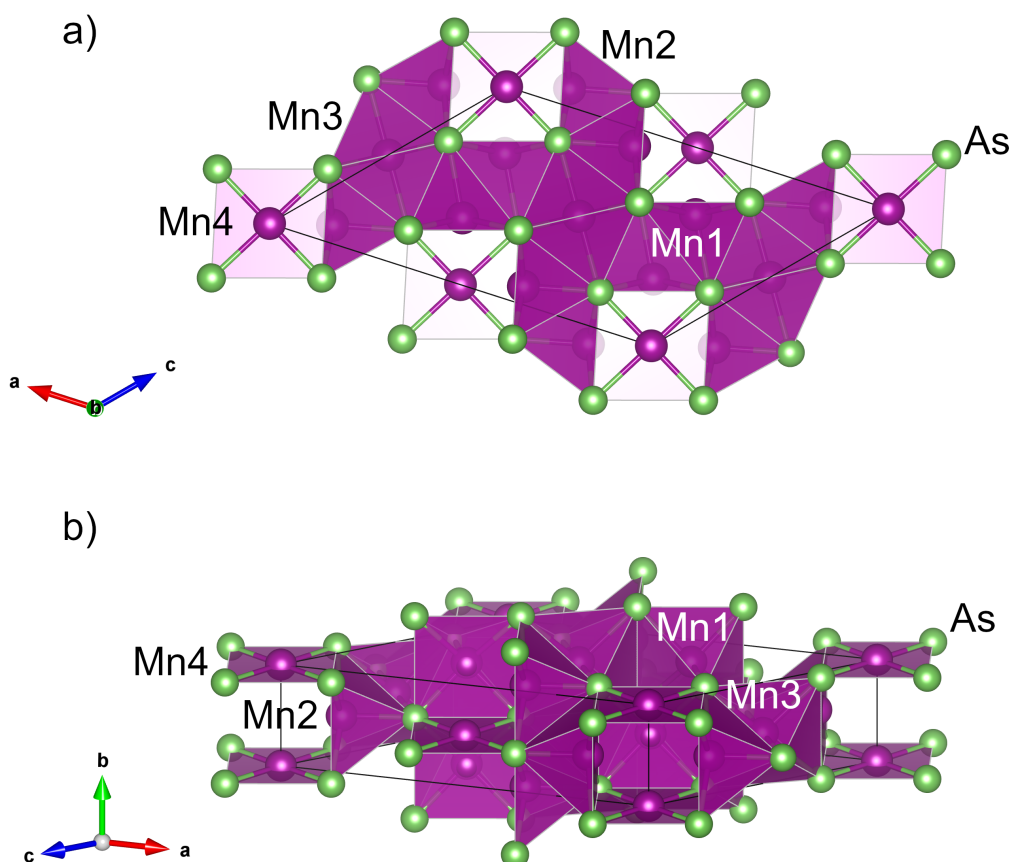


Figure 6.1: Electronic band structure

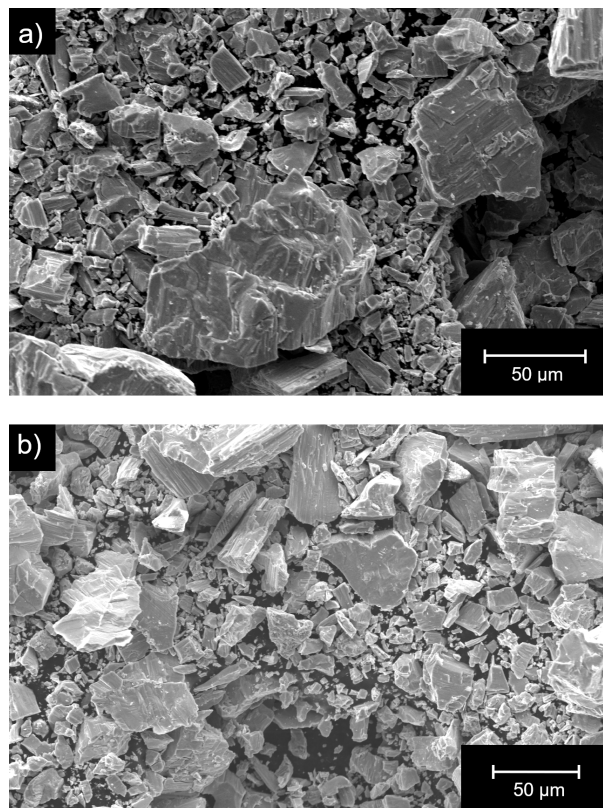


Figure 6.2: Electronic band structure

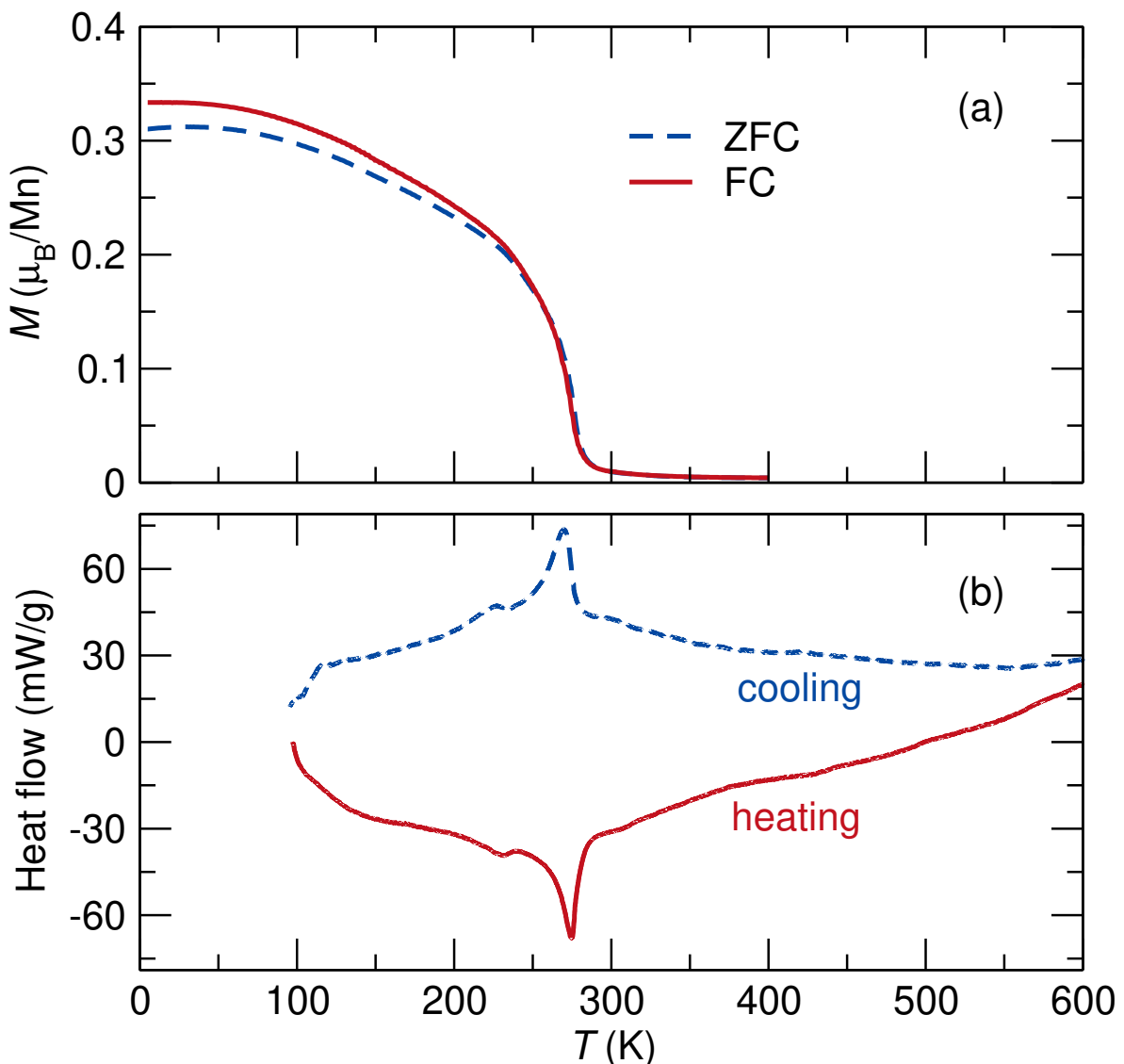


Figure 6.3: Electronic band structure

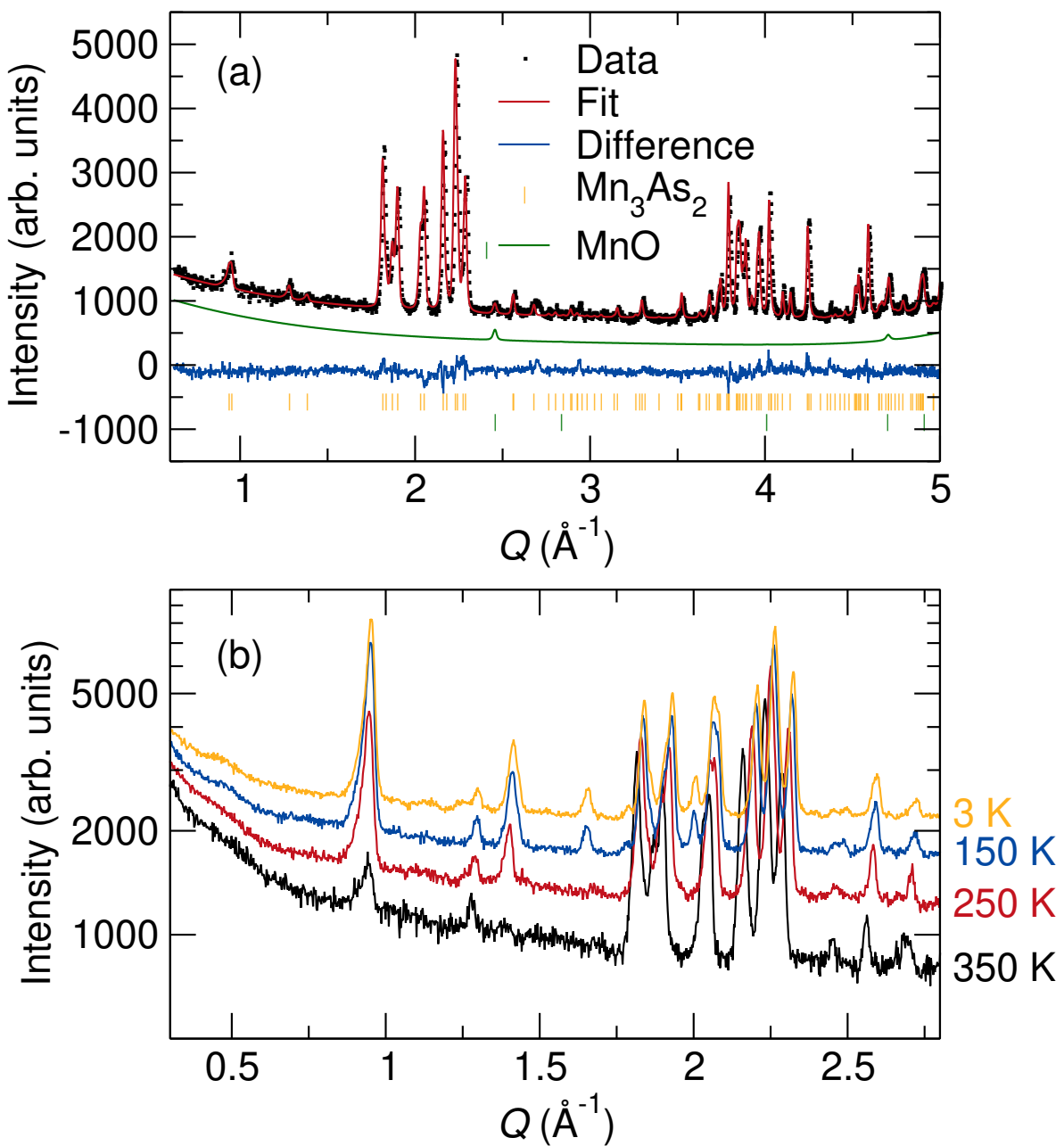


Figure 6.4: Electronic band structure

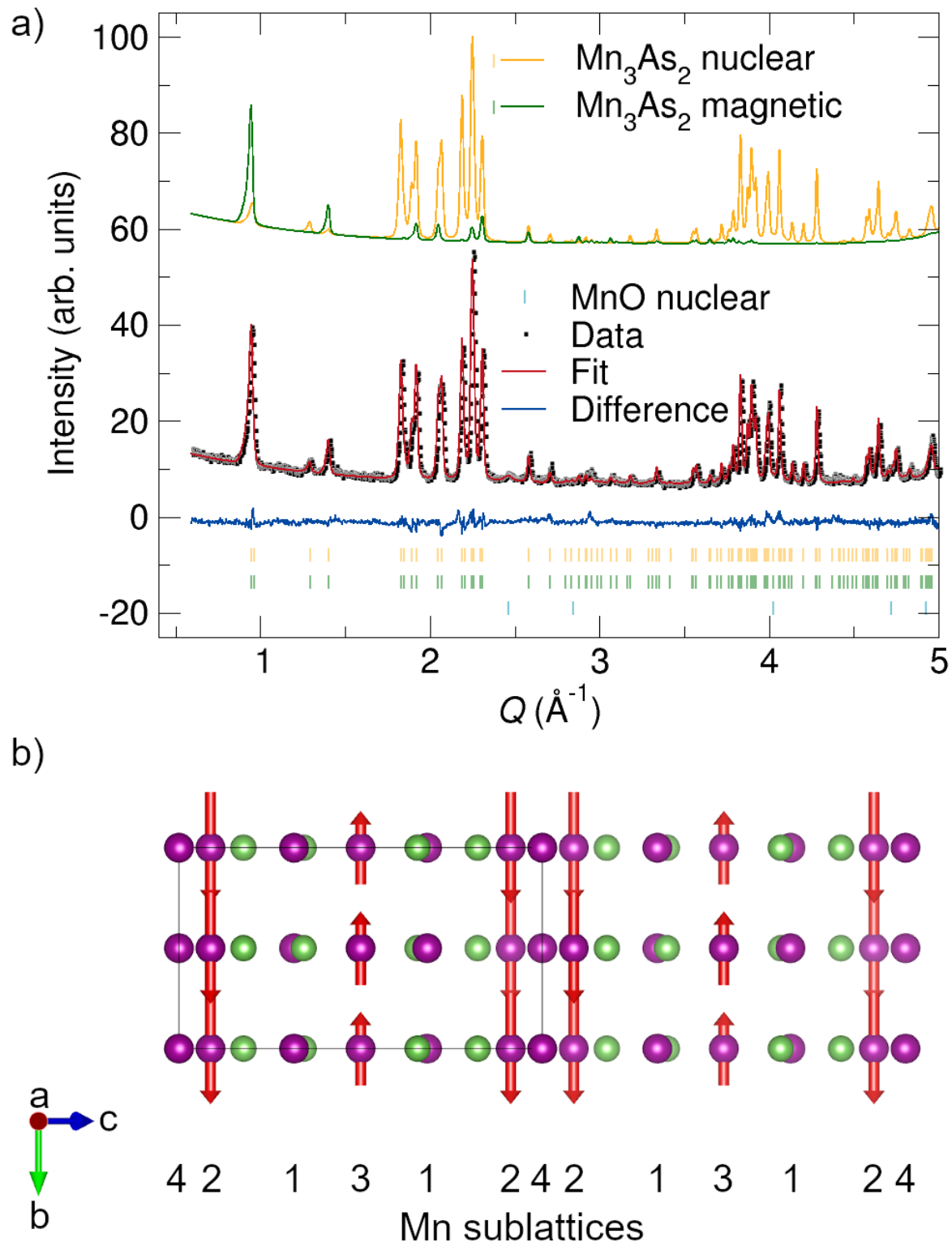


Figure 6.5: Electronic band structure

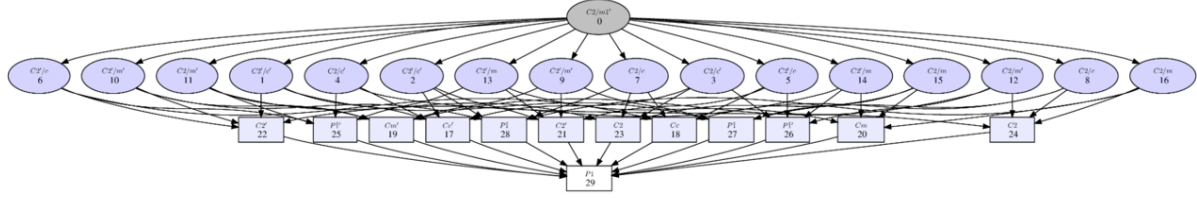


Figure 6.6: Electronic band structure

544 placerat pede. Vivamus nunc nunc, molestie ut, ultricies vel, semper in, velit. Ut porttitor.
 545 Praesent in sapien. Lorem ipsum dolor sit amet, consectetuer adipiscing elit. Duis fringilla
 546 tristique neque. Sed interdum libero ut metus. Pellentesque placerat. Nam rutrum augue
 547 a leo. Morbi sed elit sit amet ante lobortis sollicitudin. Praesent blandit blandit mauris.
 548 Praesent lectus tellus, aliquet aliquam, luctus a, egestas a, turpis. Mauris lacinia lorem sit
 549 amet ipsum. Nunc quis urna dictum turpis accumsan semper.
 550 Lorem ipsum dolor sit amet, consectetuer adipiscing elit. Etiam lobortis facilisis sem.
 551 Nullam nec mi et neque pharetra sollicitudin. Praesent imperdiet mi nec ante. Donec
 552 ullamcorper, felis non sodales commodo, lectus velit ultrices augue, a dignissim nibh lectus
 553 placerat pede. Vivamus nunc nunc, molestie ut, ultricies vel, semper in, velit. Ut porttitor.
 554 Praesent in sapien. Lorem ipsum dolor sit amet, consectetuer adipiscing elit. Duis fringilla
 555 tristique neque. Sed interdum libero ut metus. Pellentesque placerat. Nam rutrum augue
 556 a leo. Morbi sed elit sit amet ante lobortis sollicitudin. Praesent blandit blandit mauris.
 557 Praesent lectus tellus, aliquet aliquam, luctus a, egestas a, turpis. Mauris lacinia lorem sit
 558 amet ipsum. Nunc quis urna dictum turpis accumsan semper.
 559 Lorem ipsum dolor sit amet, consectetuer adipiscing elit. Etiam lobortis facilisis sem.
 560 Nullam nec mi et neque pharetra sollicitudin. Praesent imperdiet mi nec ante. Donec
 561 ullamcorper, felis non sodales commodo, lectus velit ultrices augue, a dignissim nibh lectus
 562 placerat pede. Vivamus nunc nunc, molestie ut, ultricies vel, semper in, velit. Ut porttitor.
 563 Praesent in sapien. Lorem ipsum dolor sit amet, consectetuer adipiscing elit. Duis fringilla
 564 tristique neque. Sed interdum libero ut metus. Pellentesque placerat. Nam rutrum augue
 565 a leo. Morbi sed elit sit amet ante lobortis sollicitudin. Praesent blandit blandit mauris.
 566 Praesent lectus tellus, aliquet aliquam, luctus a, egestas a, turpis. Mauris lacinia lorem sit
 567 amet ipsum. Nunc quis urna dictum turpis accumsan semper.

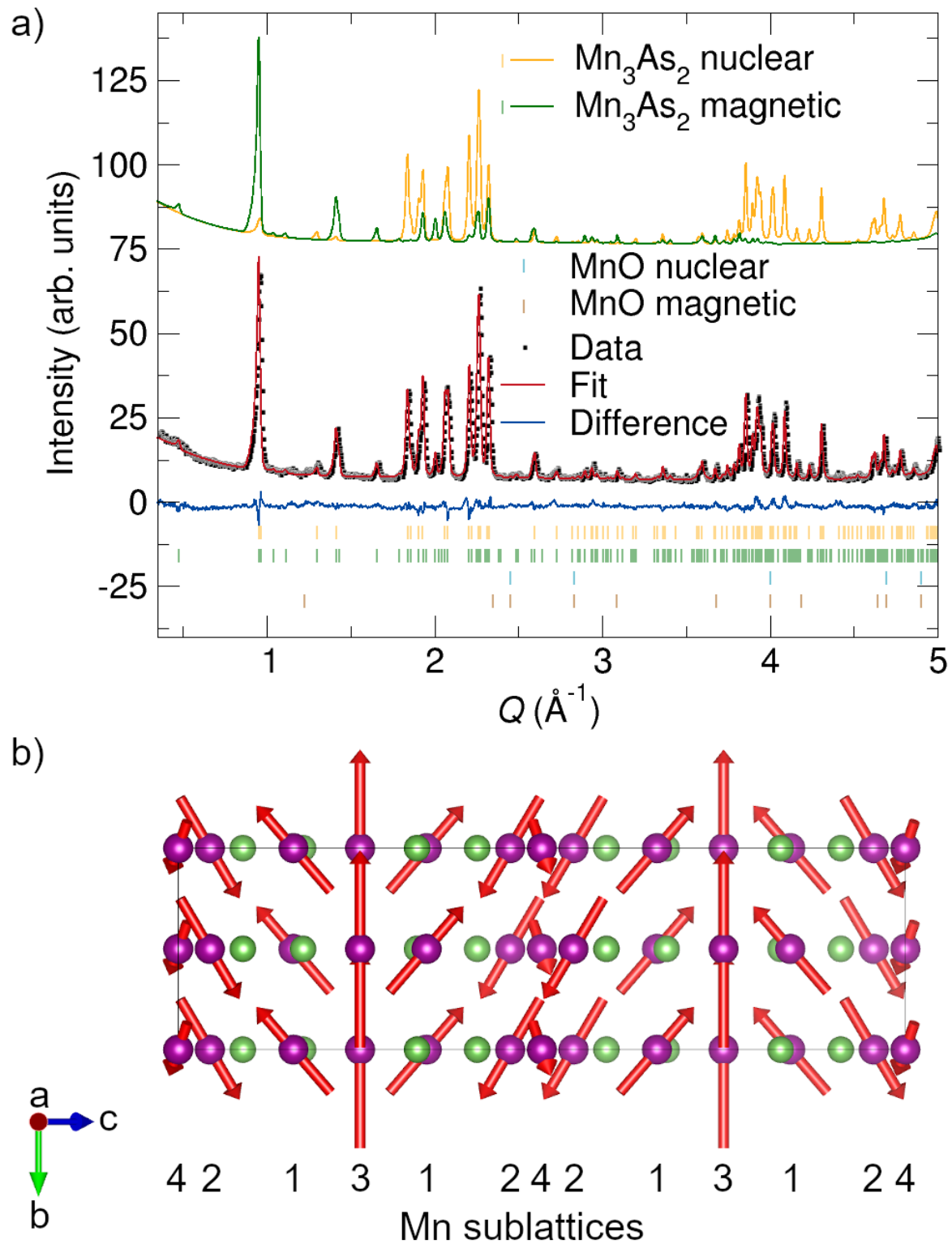


Figure 6.7: Electronic band structure

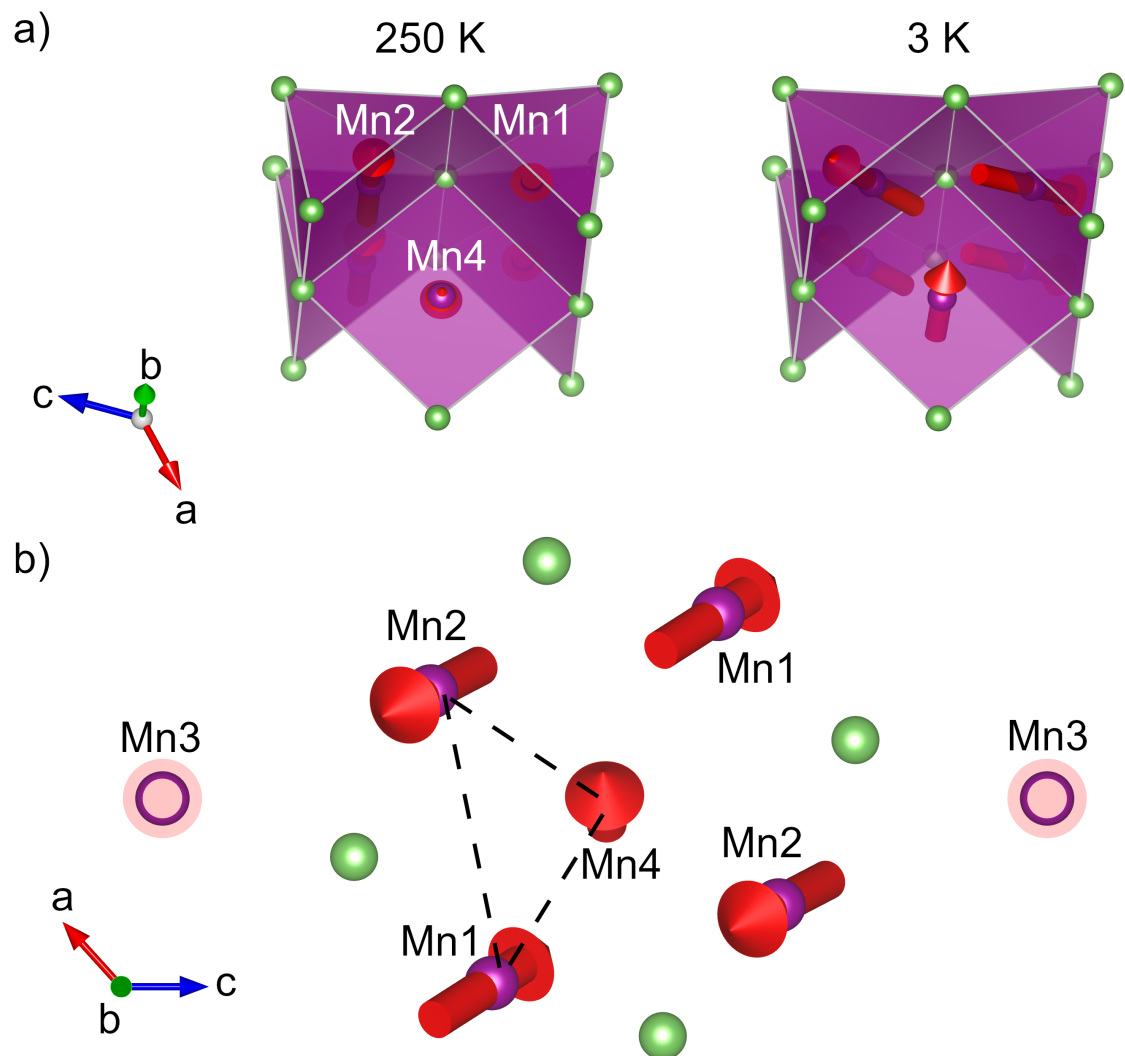


Figure 6.8: Electronic band structure

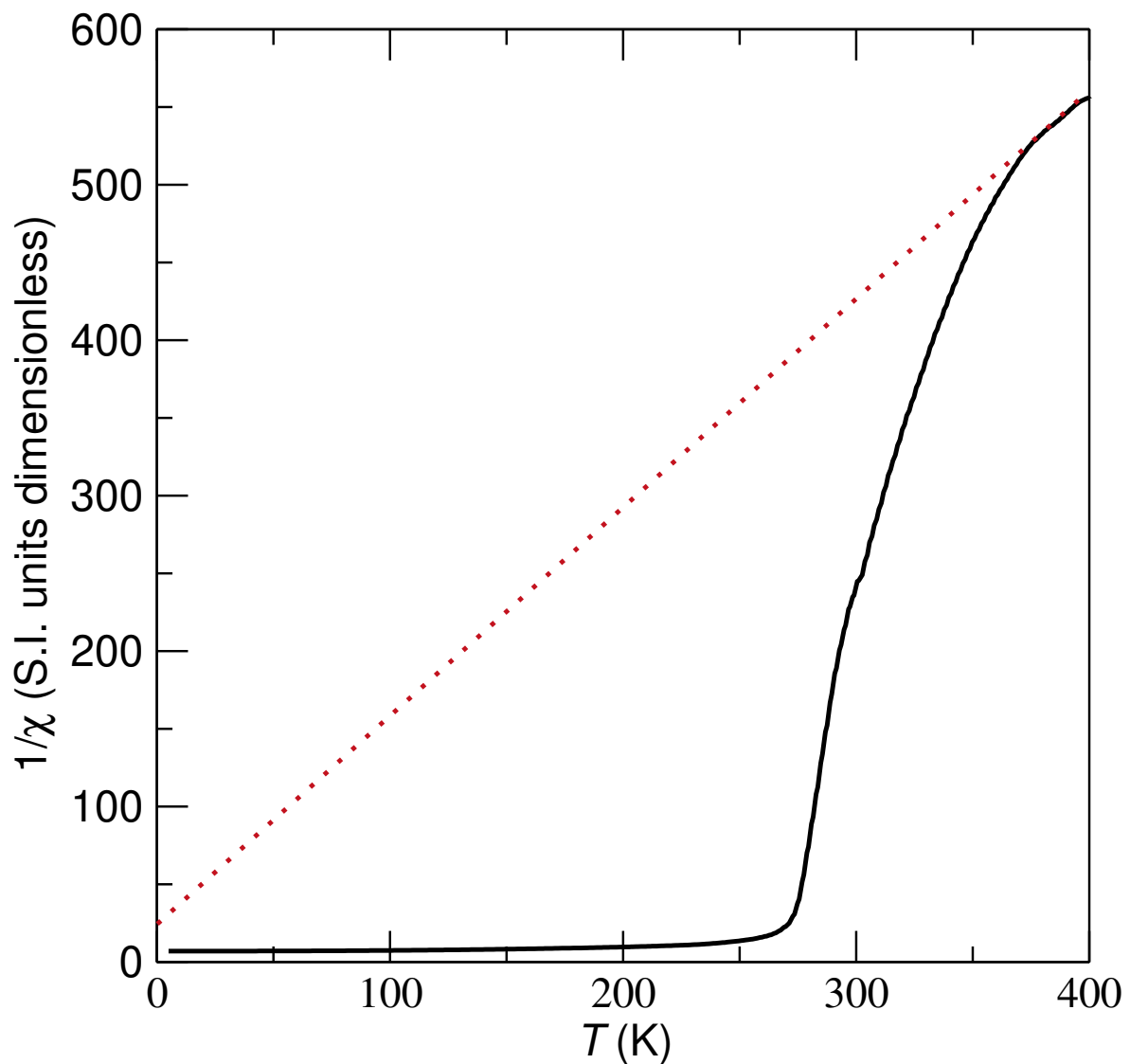


Figure 6.9: Electronic band structure

Chapter 7

Spin canting in tetragonal CuMnAs

568 Lorem ipsum dolor sit amet, consectetur adipiscing elit. Etiam lobortis facilisis sem. Nullam
569 nec mi et neque pharetra sollicitudin. Praesent imperdiet mi nec ante. Donec ullamcorper,
570 felis non sodales commodo, lectus velit ultrices augue, a dignissim nibh lectus placerat pede.
571 Vivamus nunc nunc, molestie ut, ultricies vel, semper in, velit. Ut porttitor. Praesent in sapien.
572 Lorem ipsum dolor sit amet, consectetur adipiscing elit. Duis fringilla tristique neque. Sed
573 interdum libero ut metus. Pellentesque placerat. Nam rutrum augue a leo. Morbi sed elit sit
574 amet ante lobortis sollicitudin. Praesent blandit blandit mauris. Praesent lectus tellus, aliquet
575 aliquam, luctus a, egestas a, turpis. Mauris lacinia lorem sit amet ipsum. Nunc quis urna
576 dictum turpis accumsan semper.

577 Lorem ipsum dolor sit amet, consectetur adipiscing elit. Etiam lobortis facilisis sem.
578 Nullam nec mi et neque pharetra sollicitudin. Praesent imperdiet mi nec ante. Donec
579 ullamcorper, felis non sodales commodo, lectus velit ultrices augue, a dignissim nibh lectus
580 placerat pede. Vivamus nunc nunc, molestie ut, ultricies vel, semper in, velit. Ut porttitor.
581 Praesent in sapien. Lorem ipsum dolor sit amet, consectetur adipiscing elit. Duis fringilla
582 tristique neque. Sed interdum libero ut metus. Pellentesque placerat. Nam rutrum augue
583 a leo. Morbi sed elit sit amet ante lobortis sollicitudin. Praesent blandit blandit mauris.
584 Praesent lectus tellus, aliquet aliquam, luctus a, egestas a, turpis. Mauris lacinia lorem sit
585 amet ipsum. Nunc quis urna dictum turpis accumsan semper.

586 Lorem ipsum dolor sit amet, consectetur adipiscing elit. Etiam lobortis facilisis sem.
587 Nullam nec mi et neque pharetra sollicitudin. Praesent imperdiet mi nec ante. Donec
588 ullamcorper, felis non sodales commodo, lectus velit ultrices augue, a dignissim nibh lectus
589 placerat pede. Vivamus nunc nunc, molestie ut, ultricies vel, semper in, velit. Ut porttitor.
590 Praesent in sapien. Lorem ipsum dolor sit amet, consectetur adipiscing elit. Duis fringilla
591 tristique neque. Sed interdum libero ut metus. Pellentesque placerat. Nam rutrum augue
592 a leo. Morbi sed elit sit amet ante lobortis sollicitudin. Praesent blandit blandit mauris.
593 Praesent lectus tellus, aliquet aliquam, luctus a, egestas a, turpis. Mauris lacinia lorem sit
594 amet ipsum. Nunc quis urna dictum turpis accumsan semper.

595 Lorem ipsum dolor sit amet, consectetur adipiscing elit. Etiam lobortis facilisis sem.
596 Nullam nec mi et neque pharetra sollicitudin. Praesent imperdiet mi nec ante. Donec
597 ullamcorper, felis non sodales commodo, lectus velit ultrices augue, a dignissim nibh lectus

598 placerat pede. Vivamus nunc nunc, molestie ut, ultricies vel, semper in, velit. Ut porttitor.
599 Praesent in sapien. Lorem ipsum dolor sit amet, consectetuer adipiscing elit. Duis fringilla
600 tristique neque. Sed interdum libero ut metus. Pellentesque placerat. Nam rutrum augue
601 a leo. Morbi sed elit sit amet ante lobortis sollicitudin. Praesent blandit blandit mauris.
602 Praesent lectus tellus, aliquet aliquam, luctus a, egestas a, turpis. Mauris lacinia lorem sit
603 amet ipsum. Nunc quis urna dictum turpis accumsan semper.

604 Lorem ipsum dolor sit amet, consectetuer adipiscing elit. Etiam lobortis facilisis sem.
605 Nullam nec mi et neque pharetra sollicitudin. Praesent imperdiet mi nec ante. Donec
606 ullamcorper, felis non sodales commodo, lectus velit ultrices augue, a dignissim nibh lectus
607 placerat pede. Vivamus nunc nunc, molestie ut, ultricies vel, semper in, velit. Ut porttitor.
608 Praesent in sapien. Lorem ipsum dolor sit amet, consectetuer adipiscing elit. Duis fringilla
609 tristique neque. Sed interdum libero ut metus. Pellentesque placerat. Nam rutrum augue
610 a leo. Morbi sed elit sit amet ante lobortis sollicitudin. Praesent blandit blandit mauris.
611 Praesent lectus tellus, aliquet aliquam, luctus a, egestas a, turpis. Mauris lacinia lorem sit
612 amet ipsum. Nunc quis urna dictum turpis accumsan semper.

613 Lorem ipsum dolor sit amet, consectetuer adipiscing elit. Etiam lobortis facilisis sem.
614 Nullam nec mi et neque pharetra sollicitudin. Praesent imperdiet mi nec ante. Donec
615 ullamcorper, felis non sodales commodo, lectus velit ultrices augue, a dignissim nibh lectus
616 placerat pede. Vivamus nunc nunc, molestie ut, ultricies vel, semper in, velit. Ut porttitor.
617 Praesent in sapien. Lorem ipsum dolor sit amet, consectetuer adipiscing elit. Duis fringilla
618 tristique neque. Sed interdum libero ut metus. Pellentesque placerat. Nam rutrum augue
619 a leo. Morbi sed elit sit amet ante lobortis sollicitudin. Praesent blandit blandit mauris.
620 Praesent lectus tellus, aliquet aliquam, luctus a, egestas a, turpis. Mauris lacinia lorem sit
621 amet ipsum. Nunc quis urna dictum turpis accumsan semper.

Chapter 8

Exchange interactions in Fe₂As probed by inelastic neutron scattering

622 Lorem ipsum dolor sit amet, consectetur adipiscing elit. Etiam lobortis facilisis sem. Nullam
623 nec mi et neque pharetra sollicitudin. Praesent imperdiet mi nec ante. Donec ullamcorper,
624 felis non sodales commodo, lectus velit ultrices augue, a dignissim nibh lectus placerat pede.

625 Vivamus nunc nunc, molestie ut, ultricies vel, semper in, velit. Ut porttitor. Praesent in sapien.
626 Lorem ipsum dolor sit amet, consectetur adipiscing elit. Duis fringilla tristique neque. Sed
627 interdum libero ut metus. Pellentesque placerat. Nam rutrum augue a leo. Morbi sed elit sit
628 amet ante lobortis sollicitudin. Praesent blandit blandit mauris. Praesent lectus tellus, aliquet
629 aliquam, luctus a, egestas a, turpis. Mauris lacinia lorem sit amet ipsum. Nunc quis urna
630 dictum turpis accumsan semper.

631 Lorem ipsum dolor sit amet, consectetur adipiscing elit. Etiam lobortis facilisis sem.
632 Nullam nec mi et neque pharetra sollicitudin. Praesent imperdiet mi nec ante. Donec
633 ullamcorper, felis non sodales commodo, lectus velit ultrices augue, a dignissim nibh lectus
634 placerat pede. Vivamus nunc nunc, molestie ut, ultricies vel, semper in, velit. Ut porttitor.
635 Praesent in sapien. Lorem ipsum dolor sit amet, consectetur adipiscing elit. Duis fringilla
636 tristique neque. Sed interdum libero ut metus. Pellentesque placerat. Nam rutrum augue
637 a leo. Morbi sed elit sit amet ante lobortis sollicitudin. Praesent blandit blandit mauris.
638 Praesent lectus tellus, aliquet aliquam, luctus a, egestas a, turpis. Mauris lacinia lorem sit
639 amet ipsum. Nunc quis urna dictum turpis accumsan semper.

640 Lorem ipsum dolor sit amet, consectetur adipiscing elit. Etiam lobortis facilisis sem.
641 Nullam nec mi et neque pharetra sollicitudin. Praesent imperdiet mi nec ante. Donec
642 ullamcorper, felis non sodales commodo, lectus velit ultrices augue, a dignissim nibh lectus
643 placerat pede. Vivamus nunc nunc, molestie ut, ultricies vel, semper in, velit. Ut porttitor.
644 Praesent in sapien. Lorem ipsum dolor sit amet, consectetur adipiscing elit. Duis fringilla
645 tristique neque. Sed interdum libero ut metus. Pellentesque placerat. Nam rutrum augue
646 a leo. Morbi sed elit sit amet ante lobortis sollicitudin. Praesent blandit blandit mauris.
647 Praesent lectus tellus, aliquet aliquam, luctus a, egestas a, turpis. Mauris lacinia lorem sit
648 amet ipsum. Nunc quis urna dictum turpis accumsan semper.

649 Lorem ipsum dolor sit amet, consectetur adipiscing elit. Etiam lobortis facilisis sem.
650 Nullam nec mi et neque pharetra sollicitudin. Praesent imperdiet mi nec ante. Donec
651 ullamcorper, felis non sodales commodo, lectus velit ultrices augue, a dignissim nibh lectus

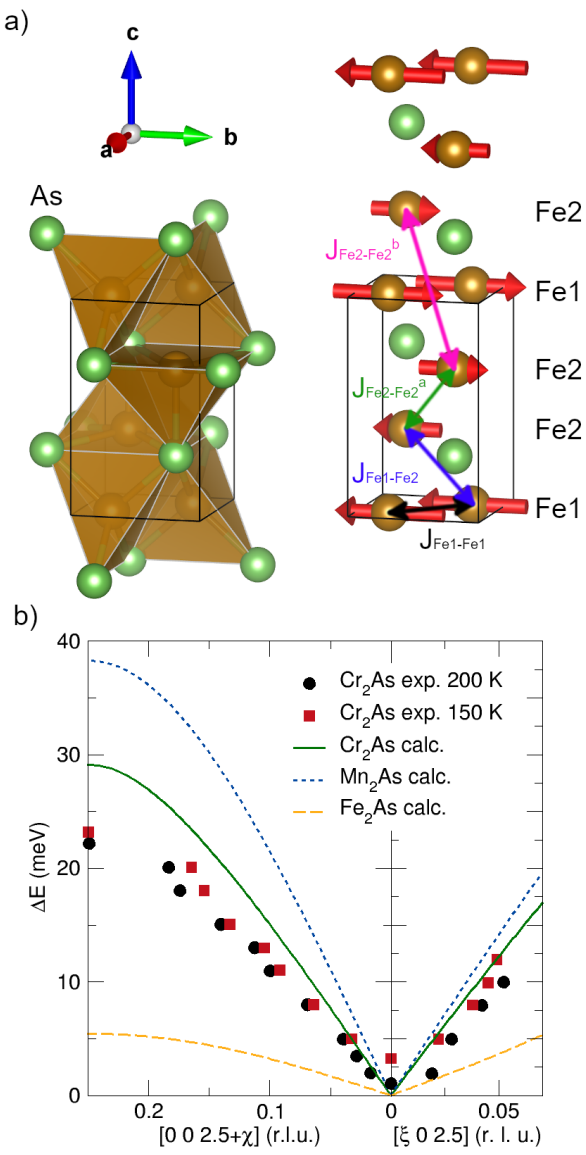


Figure 8.1: Electronic band structure



Figure 8.2: Electronic band structure

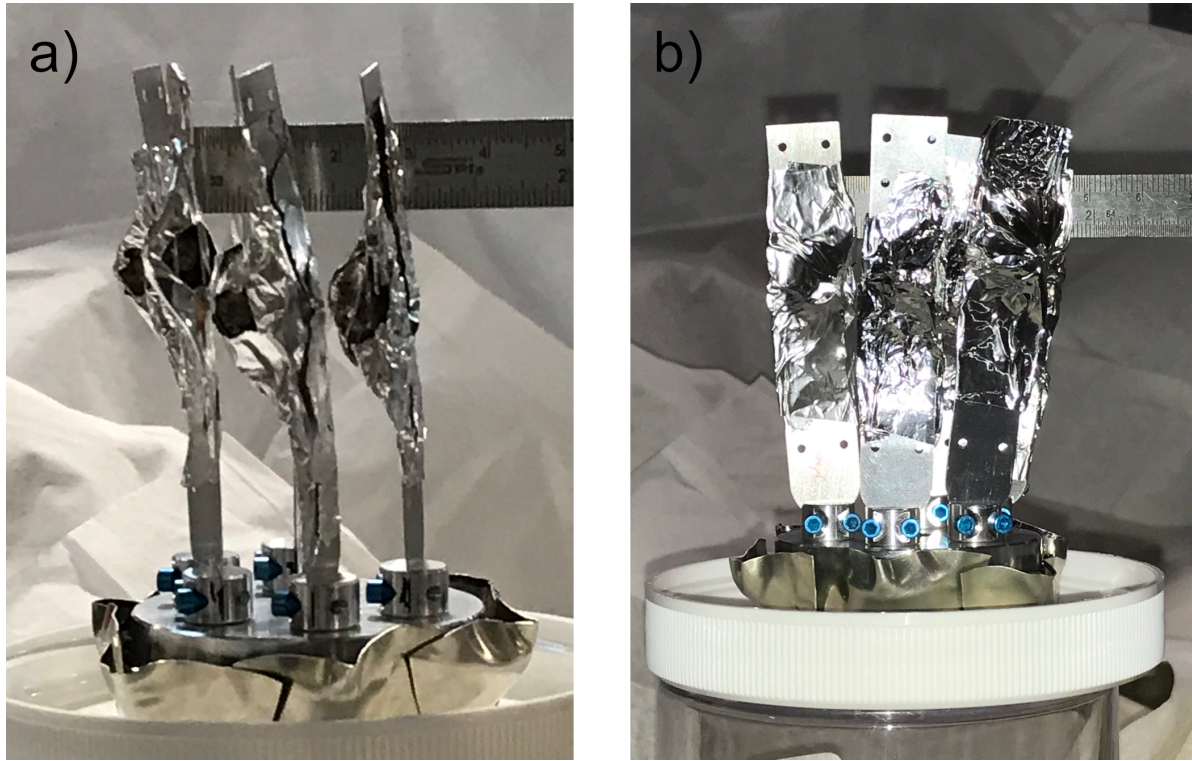


Figure 8.3: Electronic band structure

652 placerat pede. Vivamus nunc nunc, molestie ut, ultricies vel, semper in, velit. Ut porttitor.
653 Praesent in sapien. Lorem ipsum dolor sit amet, consectetuer adipiscing elit. Duis fringilla
654 tristique neque. Sed interdum libero ut metus. Pellentesque placerat. Nam rutrum augue
655 a leo. Morbi sed elit sit amet ante lobortis sollicitudin. Praesent blandit blandit mauris.
656 Praesent lectus tellus, aliquet aliquam, luctus a, egestas a, turpis. Mauris lacinia lorem sit
657 amet ipsum. Nunc quis urna dictum turpis accumsan semper.
658 Lorem ipsum dolor sit amet, consectetuer adipiscing elit. Etiam lobortis facilisis sem.
659 Nullam nec mi et neque pharetra sollicitudin. Praesent imperdiet mi nec ante. Donec
660 ullamcorper, felis non sodales commodo, lectus velit ultrices augue, a dignissim nibh lectus
661 placerat pede. Vivamus nunc nunc, molestie ut, ultricies vel, semper in, velit. Ut porttitor.
662 Praesent in sapien. Lorem ipsum dolor sit amet, consectetuer adipiscing elit. Duis fringilla
663 tristique neque. Sed interdum libero ut metus. Pellentesque placerat. Nam rutrum augue
664 a leo. Morbi sed elit sit amet ante lobortis sollicitudin. Praesent blandit blandit mauris.
665 Praesent lectus tellus, aliquet aliquam, luctus a, egestas a, turpis. Mauris lacinia lorem sit
666 amet ipsum. Nunc quis urna dictum turpis accumsan semper.
667 Lorem ipsum dolor sit amet, consectetuer adipiscing elit. Etiam lobortis facilisis sem.
668 Nullam nec mi et neque pharetra sollicitudin. Praesent imperdiet mi nec ante. Donec
669 ullamcorper, felis non sodales commodo, lectus velit ultrices augue, a dignissim nibh lectus

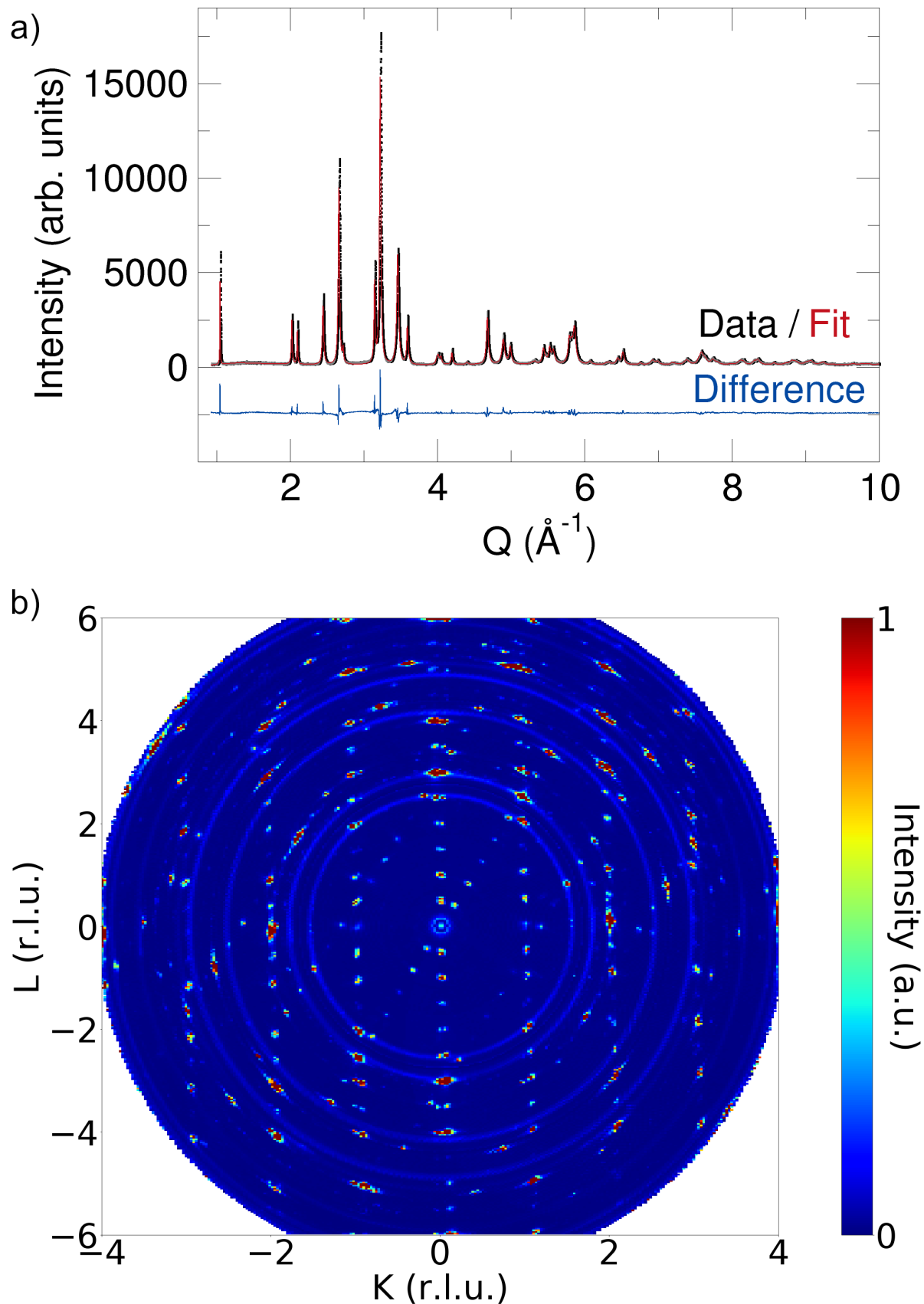


Figure 8.4: Electronic band structure

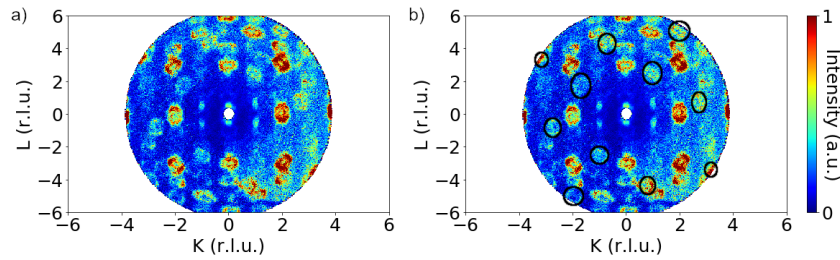


Figure 8.5: Electronic band structure

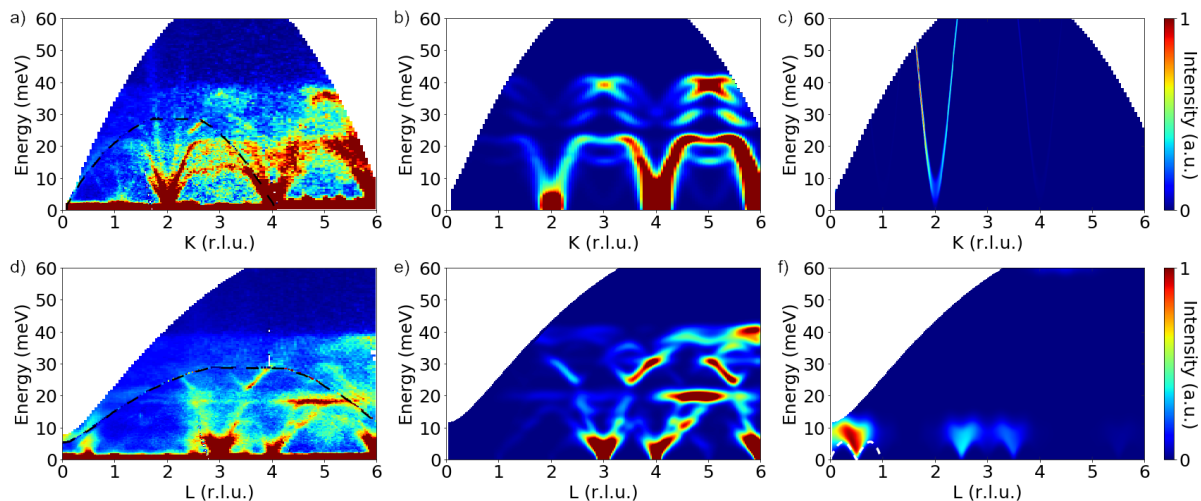


Figure 8.6: Electronic band structure

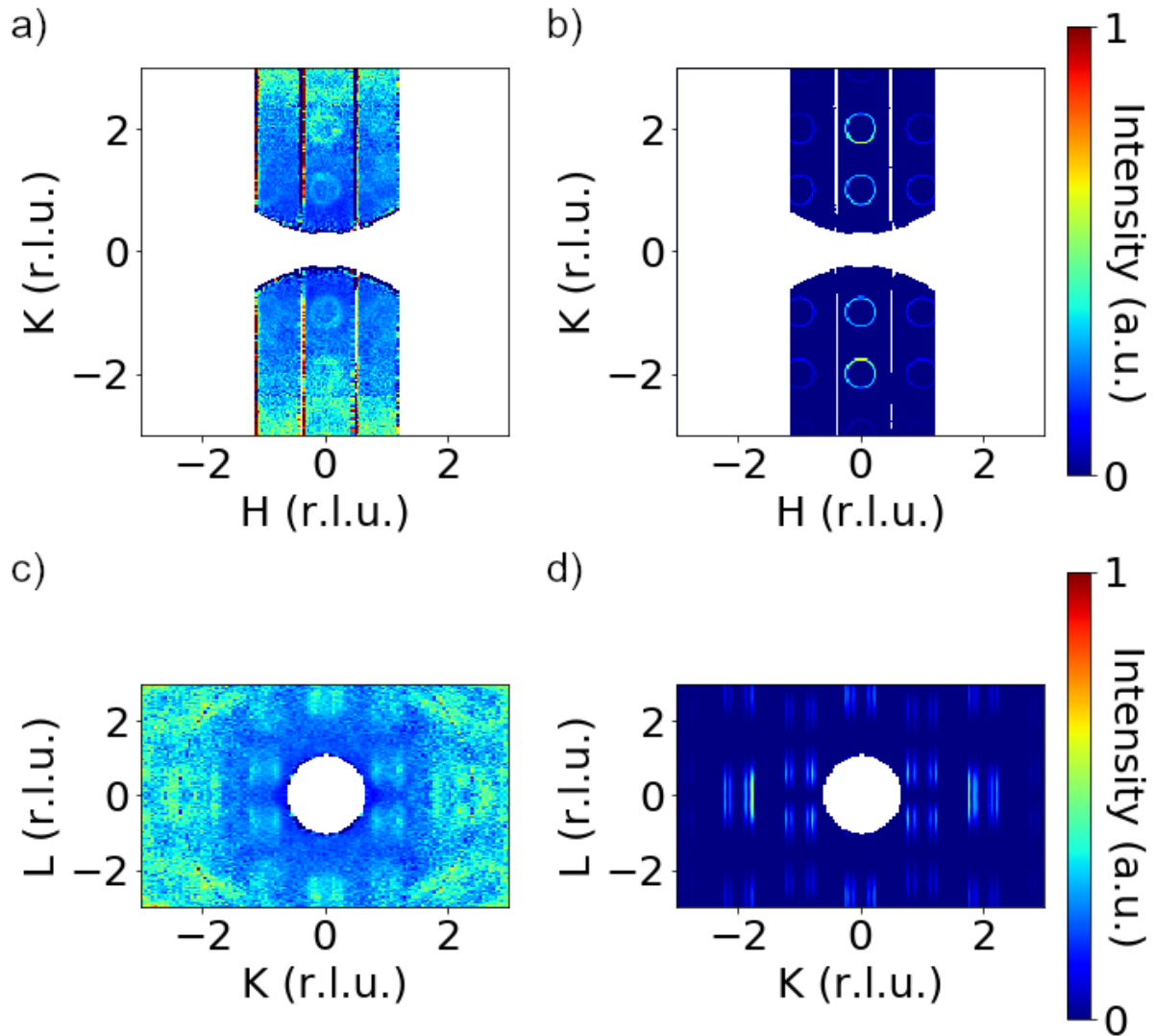


Figure 8.7: Electronic band structure

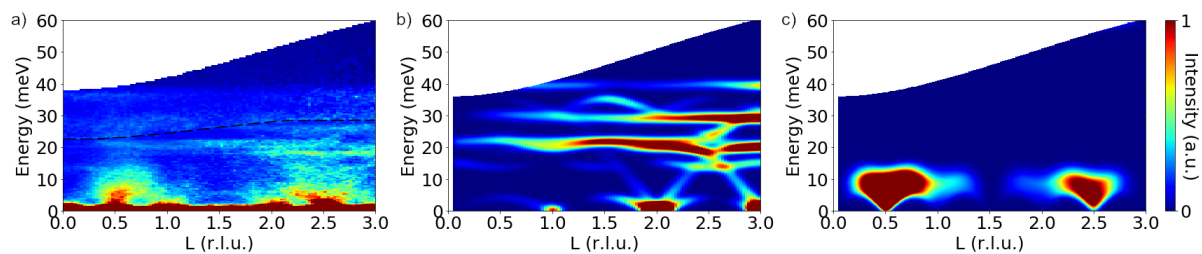


Figure 8.8: Electronic band structure

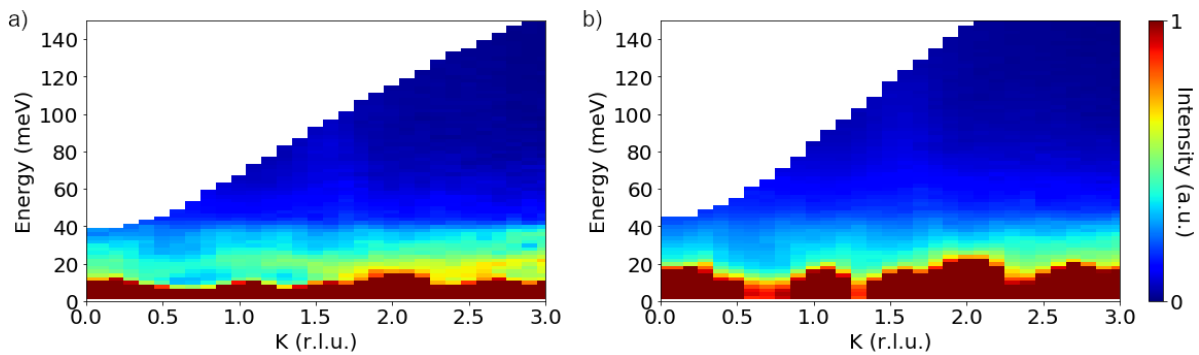


Figure 8.9: Electronic band structure

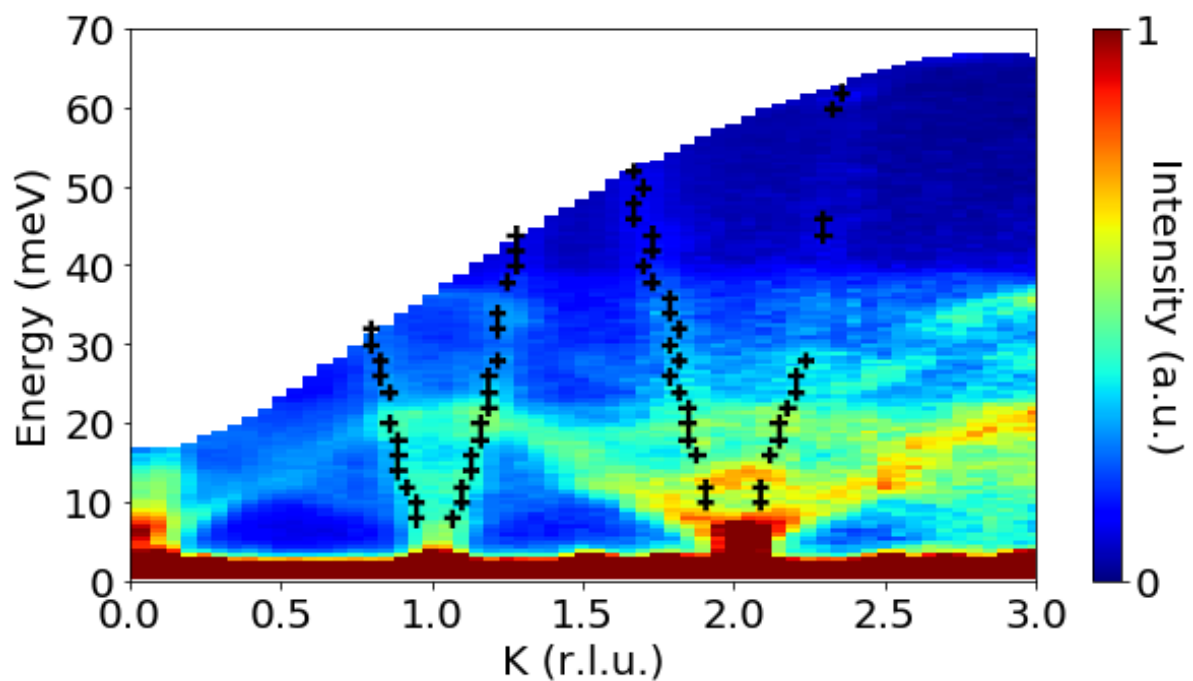


Figure 8.10: Electronic band structure

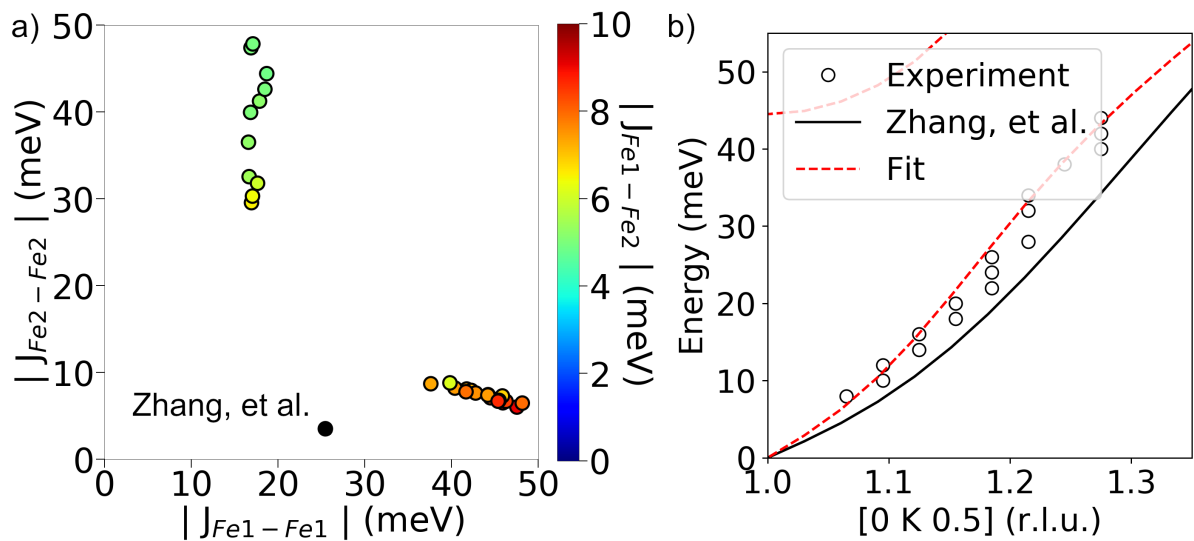


Figure 8.11: Electronic band structure

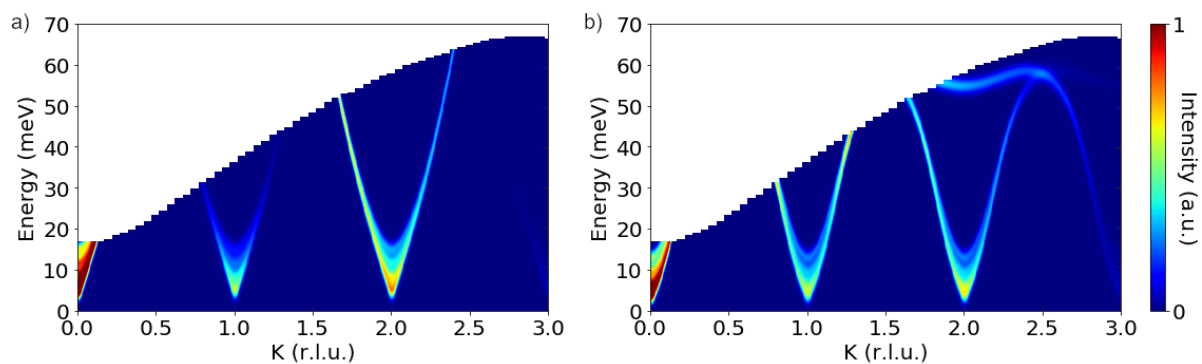


Figure 8.12: Electronic band structure

670 placerat pede. Vivamus nunc nunc, molestie ut, ultricies vel, semper in, velit. Ut porttitor.
671 Praesent in sapien. Lorem ipsum dolor sit amet, consectetuer adipiscing elit. Duis fringilla
672 tristique neque. Sed interdum libero ut metus. Pellentesque placerat. Nam rutrum augue
673 a leo. Morbi sed elit sit amet ante lobortis sollicitudin. Praesent blandit blandit mauris.
674 Praesent lectus tellus, aliquet aliquam, luctus a, egestas a, turpis. Mauris lacinia lorem sit
675 amet ipsum. Nunc quis urna dictum turpis accumsan semper.

Chapter 9

Conclusions

676 Lorem ipsum dolor sit amet, consectetur adipiscing elit. Etiam lobortis facilisis sem. Nullam
677 nec mi et neque pharetra sollicitudin. Praesent imperdiet mi nec ante. Donec ullamcorper,
678 felis non sodales commodo, lectus velit ultrices augue, a dignissim nibh lectus placerat pede.
679 Vivamus nunc nunc, molestie ut, ultricies vel, semper in, velit. Ut porttitor. Praesent in sapien.
680 Lorem ipsum dolor sit amet, consectetur adipiscing elit. Duis fringilla tristique neque. Sed
681 interdum libero ut metus. Pellentesque placerat. Nam rutrum augue a leo. Morbi sed elit sit
682 amet ante lobortis sollicitudin. Praesent blandit blandit mauris. Praesent lectus tellus, aliquet
683 aliquam, luctus a, egestas a, turpis. Mauris lacinia lorem sit amet ipsum. Nunc quis urna
684 dictum turpis accumsan semper.

685 Lorem ipsum dolor sit amet, consectetur adipiscing elit. Etiam lobortis facilisis sem.
686 Nullam nec mi et neque pharetra sollicitudin. Praesent imperdiet mi nec ante. Donec
687 ullamcorper, felis non sodales commodo, lectus velit ultrices augue, a dignissim nibh lectus
688 placerat pede. Vivamus nunc nunc, molestie ut, ultricies vel, semper in, velit. Ut porttitor.
689 Praesent in sapien. Lorem ipsum dolor sit amet, consectetur adipiscing elit. Duis fringilla
690 tristique neque. Sed interdum libero ut metus. Pellentesque placerat. Nam rutrum augue
691 a leo. Morbi sed elit sit amet ante lobortis sollicitudin. Praesent blandit blandit mauris.
692 Praesent lectus tellus, aliquet aliquam, luctus a, egestas a, turpis. Mauris lacinia lorem sit
693 amet ipsum. Nunc quis urna dictum turpis accumsan semper.

694 Lorem ipsum dolor sit amet, consectetur adipiscing elit. Etiam lobortis facilisis sem.
695 Nullam nec mi et neque pharetra sollicitudin. Praesent imperdiet mi nec ante. Donec
696 ullamcorper, felis non sodales commodo, lectus velit ultrices augue, a dignissim nibh lectus
697 placerat pede. Vivamus nunc nunc, molestie ut, ultricies vel, semper in, velit. Ut porttitor.
698 Praesent in sapien. Lorem ipsum dolor sit amet, consectetur adipiscing elit. Duis fringilla
699 tristique neque. Sed interdum libero ut metus. Pellentesque placerat. Nam rutrum augue
700 a leo. Morbi sed elit sit amet ante lobortis sollicitudin. Praesent blandit blandit mauris.
701 Praesent lectus tellus, aliquet aliquam, luctus a, egestas a, turpis. Mauris lacinia lorem sit
702 amet ipsum. Nunc quis urna dictum turpis accumsan semper.

703 Lorem ipsum dolor sit amet, consectetur adipiscing elit. Etiam lobortis facilisis sem.
704 Nullam nec mi et neque pharetra sollicitudin. Praesent imperdiet mi nec ante. Donec
705 ullamcorper, felis non sodales commodo, lectus velit ultrices augue, a dignissim nibh lectus

706 placerat pede. Vivamus nunc nunc, molestie ut, ultricies vel, semper in, velit. Ut porttitor.
707 Praesent in sapien. Lorem ipsum dolor sit amet, consectetuer adipiscing elit. Duis fringilla
708 tristique neque. Sed interdum libero ut metus. Pellentesque placerat. Nam rutrum augue
709 a leo. Morbi sed elit sit amet ante lobortis sollicitudin. Praesent blandit blandit mauris.
710 Praesent lectus tellus, aliquet aliquam, luctus a, egestas a, turpis. Mauris lacinia lorem sit
711 amet ipsum. Nunc quis urna dictum turpis accumsan semper.

712 Lorem ipsum dolor sit amet, consectetuer adipiscing elit. Etiam lobortis facilisis sem.
713 Nullam nec mi et neque pharetra sollicitudin. Praesent imperdiet mi nec ante. Donec
714 ullamcorper, felis non sodales commodo, lectus velit ultrices augue, a dignissim nibh lectus
715 placerat pede. Vivamus nunc nunc, molestie ut, ultricies vel, semper in, velit. Ut porttitor.
716 Praesent in sapien. Lorem ipsum dolor sit amet, consectetuer adipiscing elit. Duis fringilla
717 tristique neque. Sed interdum libero ut metus. Pellentesque placerat. Nam rutrum augue
718 a leo. Morbi sed elit sit amet ante lobortis sollicitudin. Praesent blandit blandit mauris.
719 Praesent lectus tellus, aliquet aliquam, luctus a, egestas a, turpis. Mauris lacinia lorem sit
720 amet ipsum. Nunc quis urna dictum turpis accumsan semper.

721 Lorem ipsum dolor sit amet, consectetuer adipiscing elit. Etiam lobortis facilisis sem.
722 Nullam nec mi et neque pharetra sollicitudin. Praesent imperdiet mi nec ante. Donec
723 ullamcorper, felis non sodales commodo, lectus velit ultrices augue, a dignissim nibh lectus
724 placerat pede. Vivamus nunc nunc, molestie ut, ultricies vel, semper in, velit. Ut porttitor.
725 Praesent in sapien. Lorem ipsum dolor sit amet, consectetuer adipiscing elit. Duis fringilla
726 tristique neque. Sed interdum libero ut metus. Pellentesque placerat. Nam rutrum augue
727 a leo. Morbi sed elit sit amet ante lobortis sollicitudin. Praesent blandit blandit mauris.
728 Praesent lectus tellus, aliquet aliquam, luctus a, egestas a, turpis. Mauris lacinia lorem sit
729 amet ipsum. Nunc quis urna dictum turpis accumsan semper.

References

- [1] W. Toy and B. Zee, *Computer Hardware/Software Architecture*, vol. First Edit. 1986.
- [2] J. S. Meena, S. M. Sze, U. Chand, and T. Y. Tseng, "Overview of emerging nonvolatile memory technologies," *Nanoscale Research Letters*, vol. 9, pp. 1–33, 2014.
- [3] K. M. Krishnan, *Fundamentals and Applications of Magnetic Materials*, vol. First Edit. 2016.
- [4] P. Wadley, B. Howells, J. Zelezny, C. Andrews, V. Hills, R. P. Campion, V. Novak, K. Olejnik, F. Maccherozzi, S. S. Dhesi, S. Y. Martin, T. Wagner, J. Wunderlich, F. Freimuth, Y. Mokrousov, J. Kunes, J. S. Chauhan, M. J. Grzybowski, A. W. Rushforth, K. W. Edmonds, B. L. Gallagher, and T. Jungwirth, "Electrical switching of an antiferromagnet," *Science*, vol. 351, pp. 587–591, 2016.
- [5] C. Chappert, A. Fert, and F. N. Van Dau, "The emergence of spin electronics in data storage," *Nature Materials*, vol. 6, pp. 813–823, 2007.
- [6] S. Bhatti, R. Sbiaa, A. Hirohata, H. Ohno, S. Fukami, and S. N. Piramanayagam, "Spintronics based random access memory: a review," *Materials Today*, vol. 20, pp. 530–548, 2017.
- [7] H. V. Gomonay and V. M. Loktev, "Spin transfer and current-induced switching in antiferromagnets," *Physical Review B - Condensed Matter and Materials Physics*, vol. 81, p. 144427, 2010.
- [8] S. A. Siddiqui, J. Sklenar, K. Kang, M. J. Gilbert, A. Schleife, N. Mason, and A. Hoffmann, "Metallic antiferromagnets," *Journal of Applied Physics*, vol. 128, p. 040904, 2020.
- [9] A. Manchon and S. Zhang, "Theory of nonequilibrium intrinsic spin torque in a single nanomagnet," *Physical Review B - Condensed Matter and Materials Physics*, vol. 78, p. 212405, 2008.
- [10] J. Železný, H. Gao, K. Výborný, J. Zemen, J. Mašek, A. Manchon, J. Wunderlich, J. Sinova, and T. Jungwirth, "Relativistic néel-order fields induced by electrical current in antiferromagnets," *Physical Review Letters*, vol. 113, no. 15, pp. 1–5, 2014.
- [11] J. Železný, H. Gao, A. Manchon, F. Freimuth, Y. Mokrousov, J. Zemen, J. Mašek, J. Sinova, and T. Jungwirth, "Spin-orbit torques in locally and globally noncentrosymmetric crystals: Antiferromagnets and ferromagnets," *Physical Review B*, vol. 95, p. 014403, 2017.

- [12] M. Meinert, D. Graulich, and T. Matalla-wagner, "Electrical Switching of Antiferromagnetic Mn₂Au and the Role of Thermal Activation," *Physical Review Applied*, vol. 9, p. 64040, 2018.
- [13] T. Matalla-Wagner, M. F. Rath, D. Graulich, J. M. Schmalhorst, G. Reiss, and M. Meinert, "Electrical Neél-Order Switching in Magnetron-Sputtered CuMnAs Thin Films," *Physical Review Applied*, vol. 12, p. 064003, 2019.
- [14] Y. Kim, K. Kang, A. Schleife, and M. J. Gilbert, "Voltage-induced switching of an antiferromagnetically ordered topological Dirac semimetal," *Physical Review B*, vol. 97, p. 134415, 2018.
- [15] A. N. Nateprov, V. C. Kravtsov, V. Fritsch, and H. von Löhneysen, "Structure and properties of the tetragonal phase of MnCuAs," *Surface Engineering and Applied Electrochemistry*, vol. 47, pp. 540–543, 2011.
- [16] F. MáčA, J. Mašek, O. Stelmakhovych, X. Martí, H. Reichlová, K. Uhlířová, P. Beran, P. Wadley, V. Novák, and T. Jungwirth, "Room-temperature antiferromagnetism in CuMnAs," *Journal of Magnetism and Magnetic Materials*, vol. 324, pp. 1606–1612, 2012.
- [17] P. Wadley, V. Novák, R. P. Campion, C. Rinaldi, X. Martí, H. Reichlová, J. Zelezny, J. Gazquez, M. A. Roldan, M. Varela, D. Khalyavin, S. Langridge, D. Kriegner, F. Máca, J. Masek, R. Bertacco, V. Holy, A. W. Rushforth, K. W. Edmonds, B. L. Gallagher, C. T. Foxon, J. Wunderlich, and T. Jungwirth, "Tetragonal phase of epitaxial room-temperature antiferromagnet CuMnAs," *Nature Communications*, vol. 4, p. 2322, 2013.
- [18] K. Uhlirova, R. Tarasenko, F. J. Martinez-Casado, B. Vondrackova, and Z. Matej, "Synthesis and single crystal study of CuMn₃As₂ and Cu₂Mn₄As₃," *Journal of Alloys and Compounds*, vol. 650, pp. 224–227, 2015.
- [19] V. Hills, P. Wadley, R. P. Campion, V. Novak, R. Beardsley, K. W. Edmonds, B. L. Gallagher, B. Ouladdiaf, and T. Jungwirth, "Paramagnetic to antiferromagnetic transition in epitaxial tetragonal CuMnAs (invited)," *Journal of Applied Physics*, vol. 117, p. 172608, 2015.
- [20] P. Wadley, V. Hills, M. R. Shahedkhah, K. W. Edmonds, R. P. Campion, V. Novák, B. Ouladdiaf, D. Khalyavin, S. Langridge, V. Saidl, P. Nemec, A. W. Rushforth, B. L. Gallagher, S. S. Dhesi, F. MacCherozzi, J. Železný, and T. Jungwirth, "Antiferromagnetic structure in tetragonal CuMnAs thin films," *Scientific Reports*, vol. 5, p. 17079, 2015.
- [21] A. E. Austin, E. Adelson, and W. H. Cloud, "Magnetic Structures of Mn₂As and Mn₂Sb_{0.7}As_{0.3}," *Journal of Applied Physics*, vol. 33, pp. 1356–1357, 1962.
- [22] G. E. Bacon and R. Street, "Magnetic Structure of Manganse Arsenide," *Nature*, vol. 175, p. 518, 1955.
- [23] "Magnetic ordering and metal-atom site preference in tetragonal CrMnAs: Electronic correlation effects," *Journal of Computational Chemistry*, vol. 39, pp. 1585–1593, 2018.
- [24] Y. Zhang, J. Brgoch, and G. J. Miller, "Magnetic ordering in tetragonal 3d metal arsenides M₂As (M = Cr, Mn, Fe): An ab initio investigation," *Inorganic Chemistry*, vol. 52, pp. 3013–3021, 2013.

- [25] Y. Zhang and G. J. Miller, "Competition between direct and indirect exchange couplings in MnFeAs: A first-principles investigation," *Journal of Physical Chemistry C*, vol. 119, pp. 580–589, 2015.
- [26] X. Zhang, Q. Liu, J.-W. Luo, A. J. Freeman, and A. Zunger, "Hidden spin polarization in inversion-symmetric bulk crystals," *Nature Physics*, vol. 10, pp. 387–393, 2014.
- [27] S. Y. Bodnar, M. Filianina, S. P. Bommanaboyena, T. Forrest, F. Maccherozzi, A. A. Sapozhnik, Y. Skourski, M. Kläui, and M. Jourdan, "Imaging of current induced Néel vector switching in antiferromagnetic Mn₂Au," *Physical Review B*, vol. 99, pp. 8–12, 2019.
- [28] M. A. Susner, D. S. Parker, and A. S. Sefat, "Importance of doping and frustration in itinerant Fe-doped Cr₂Al," *Journal of Magnetism and Magnetic Materials*, vol. 392, pp. 68–73, 2015.
- [29] M. Atoji, "Antiferromagnetic structure of AlCr₂," *The Journal of Chemical Physics*, vol. 43, pp. 222–225, 1965.
- [30] A. Kallel and F. D. Bergevin, "ANTIFERROMAGNETISME DE LA SOLUTION SOLIDE DE L'ALUMINTUM DANS LE CHROME," *Solid State Communications*, vol. 5, pp. 955–958, 1967.
- [31] G. Venturini, R. Welter, and B. Malaman, "Crystallographic data and magnetic properties of RT₆Ge₆ compounds (R Sc, Y, Nd, Sm, GdLu; TMn, Fe)," *Journal of Alloys and Compounds*, vol. 185, pp. 99–107, 1992.
- [32] T. Mazet, O. Isnard, and B. Malaman, "Neutron diffraction and 57Fe Mössbauer study of the HfFe₆Ge₆-type RFe₆Ge₆ compounds (R = Sc , Ti , Zr , Hf , Nb)," *Solid State Communications*, vol. 114, pp. 91–96, 2000.
- [33] S. Nakatsuji, N. Kiyohara, and T. Higo, "Large anomalous Hall effect in a non-collinear antiferromagnet at room temperature," *Nature*, vol. 527, pp. 212–215, 2015.
- [34] J. Kübler and C. Felser, "Non-collinear antiferromagnets and the anomalous Hall effect," *Epl*, vol. 108, p. 67001, 2014.
- [35] M. Kimata, H. Chen, K. Kondou, S. Sugimoto, P. K. Muduli, M. Ikhlas, Y. Omori, T. Tomita, A. H. MacDonald, S. Nakatsuji, and Y. Otani, "Magnetic and magnetic inverse spin Hall effects in a non-collinear antiferromagnet," *Nature*, vol. 565, pp. 627–630, 2019.
- [36] U. Häussermann, M. Boström, P. Viklund, R. Ö, and T. Björnängen, "FeGa₃ and RuGa₃: Semiconducting intermetallic compounds," *Journal of Solid State Chemistry*, vol. 165, pp. 94–99, 2002.
- [37] P. Viklund, S. Lidin, P. Berastegui, and U. Häussermann, "Variations of the FeGa₃ structure type in the systems CoIn_{3-x}Zn_x and CoGa_{3-x}ZN_x," *Journal of Solid State Chemistry*, vol. 165, pp. 100–110, 2002.
- [38] Y. Zhang, C. Michioka, M. Imai, H. Ueda, and K. Yoshimura, "Effect of Co substitution on the magnetic properties in Fe_{1-x}CoxGa₃," *Journal of Physics: Conference Series*, vol. 868, p. 012025, 2017.

- [39] D. Harker, "The crystal structure of Ni₄Mo," *The Journal of Chemical Physics*, vol. 12, pp. 315–317, 1944.
- [40] A. Taylor and N. J. Doyle, "Further studies on the nickel–aluminium system. I. β -NiAl and δ -Ni₂Al₃ phase fields," *Journal of Applied Crystallography*, vol. 5, pp. 201–209, 1972.
- [41] M. Yuzuri and M. Yamada, "On the Magnetic Properties of the Compound Mn₂As," *Journal of the Physical Society of Japan*, vol. 15, pp. 1845–1850, 1960.
- [42] K. Uhlirova, E. Duverger-Nedellec, R. H. Colman, J. Volny, B. Vondrackova, and K. Carva, "The stability and physical properties of the tetragonal phase of bulk CuMnAs antiferromagnet," *Journal of Alloys and Compounds*, vol. 771, pp. 680–685, 2019.
- [43] A. A. Coelho, "TOPAS and TOPAS-Academic: an optimization program integrating computer algebra and crystallographic objects written in C++," *Journal of Applied Crystallography*, vol. 51, pp. 210–218, 2018.
- [44] B. H. Toby and R. B. Von Dreele, "GSAS-II: the genesis of a modern open-source all purpose crystallography software package," *Journal of Applied Crystallography*, vol. 46, pp. 544–549, 2013.